IEEE Access
Multidisciplinary | Rapid Review | Open Access Journal

Received 18 April 2024, accepted 20 May 2024, date of publication 27 May 2024, date of current version 3 June 2024.

Digital Object Identifier 10.1109/ACCESS.2024.3406248

RESEARCH ARTICLE

Optimal Location of Cellular Base Stations via Convex Optimization: An Analytical Framework and Numerical Algorithms

ELHAM KALANTARI[1], SERGEY LOYKA[1], (Senior Member, IEEE), AND HALIM YANIKOMEROGLU[2], (Fellow, IEEE)

[1]School of Electrical Engineering and Computer Science, University of Ottawa, Ottawa, ON K1N 6N5, Canada

[2]Department of Systems and Computer Engineering, Carleton University, Ottawa, ON K1S 5B6, Canada

Corresponding author: Sergey Loyka (sergey.loyka@uottawa.ca)

ABSTRACT A novel analytical approach to optimal base station (BS) location problem is proposed. It is based on the widely used system and propagation path models but, unlike known studies, makes use a convex optimization formulation to minimize the total transmit power subject to quality-of-service (QoS, rate) constraints. In contrast to the previously-proposed approaches, the sufficient Karush-Kuhn-Tucker (KKT) conditions are used here to characterize a *globally* (rather than locally)-optimum point as a convex combination of user locations, where convex weights depend on user parameters, path loss exponent and overall geometry of the problem. Based on this characterization, a number of novel closed-form solutions are obtained. In particular, the optimum BS location is shown to be the average of user locations in the case of unobstructed line-of-sight (LOS) propagation (the path loss exponent equals 2) and identical user parameters but not in general. If the user set is symmetric, the optimal BS location is independent of the pathloss exponent, which is not the case in general. The analytical results show the impact of propagation conditions (e.g. clear/obstructed LOS) as well as system and user parameters (bandwidth, rate demand, etc.) on optimal BS location: the higher the path loss exponent, the heavier the impact of distant users; users with higher rate demands have more impact. The obtained analytical results facilitate insights, which are unavailable from purely numerical studies and which can be used to develop design guidelines. Based on these results, an iterative algorithm is proposed and its convergence is proved. The single BS results are further extended to multi-BS scenarios (e.g. a cell cluster) using the K-means algorithm with proper modifications, so that the total (sum) BS power in a cell cluster is locally minimized, subject to user rate constrains. Numerical experiments validate the analytical solutions and show the effectiveness of the proposed algorithms. Overall, the emphasis is on an analytical framework, solutions and insights rather than on numerical algorithms.

INDEX TERMS Wireless communication, cellular base station, unmanned aerial vehicle (UAV), optimal location, convex optimization, global optimum, quality-of-service, KKT conditions, K-means algorithm.

I. INTRODUCTION

With the explosive growth of wireless traffic demands and due to high costs and scarcity of radio spectrum resources, cell planning is of major importance for wireless service providers. It includes determining optimum locations and the number of base stations (BSs) to meet the traffic and quality-of-service (QoS) requirements at minimum cost [1]. Communication technologies are currently responsible for around 5% of the total generated carbon footprint and this amount is expected to increase significantly with full deployment of 5G systems and with the introduction of

The associate editor coordinating the review of this manuscript and approving it for publication was Yafei Hou.

newly-developed 6G systems since the data traffic and the number of connected devices will increase significantly. This calls for energy-efficient approach to wireless communications, which already became an active area of research [2], [3]. In this paper, we address the energy efficiency and also inter-cell interference issues by optimizing a cellular base station location to minimize its total transmit (Tx) power (to all users) and finding an optimal power allocation among users subject to rate constraints for each user, which represent QoS requirements.

A. TERRESTRIAL BS LOCATION

The problem of BS location in cellular networks has been extensively studied in the existing literature [4], [5], [6], [7], [8], [9], [10], [11], [12], [13], [14], [15], [16], [17]. A large number of optimization algorithms have been proposed to attack this problem numerically, taking into account a number of practically-important parameters and limitations. Many of the proposed algorithms use a pre-selected finite list of candidate sites where the BS could potentially be located and look for ones that optimize some objective function amongst that list [4], [5], [6], [7], [8], [9], [10]. The considered problems are formulated as mixed integer programming or combinatorial optimization and the methods to solve them include simulated annealing [5], Tabu search [4], [6] [9], simplex method and branch and bound algorithm [8], etc. While these approaches can be useful in practice, their common feature is that the considered problems are NP-hard (i.e. the numerical complexity grows exponentially fast with the problem size), and convergence of algorithms to a global optimum cannot be guaranteed, due to the lack of convexity of the underlying optimization problems. Furthermore, the sub-optimality gap is also unknown. Due to the nature of numerical algorithms, they offer limited insight into the problem, for which no analytical solution is known either.

A different approach is adopted in [11] and [12], where an optimal BS location is searched over the whole area of interest (without assuming a finite number of candidate locations). Additionally, after finding sub-optimal BS locations, the number of BSs is minimized by removing redundant BSs so that the quality of network service is not affected. Numerical algorithms are proposed for this two-stage optimization process. A pattern search algorithm is used in [11] to minimize the total power consumption of the network by properly locating BSs subject to the SIR constraints. It is based on the mesh-adaptive direct search extended to include non-linear inequalities via the augmented Lagrangian. While the algorithm converges to a Karush-Kuhn-Tucker (KKT) point, this is not sufficient for global optimality since the underlying optimization problem is not convex (so that a KKT point can be a local rather than global minimum, an inflection point, or even a maximum rather than minimum). A combinatorial optimization problem is formulated in [12] to find BS locations that satisfy area coverage and cell capacity constraints. Two heuristic numerical algorithms, namely particle swarm optimization and gray-wolf optimization, are used and afterward the redundant BSs are eliminated to achieve the minimum required number of BSs. Although these algorithms can be useful in practice, their convergence to a globally-optimal solution is not guaranteed and their numerical complexity can be prohibitively large for a large problem size.

Yet another approach is adopted in [13] and [14], where the weighted sum pathloss (to all users) is minimized by properly locating a base station. Various numerical algorithms for local optimization are used, such as Hooke-Jeeves', quasi-Newton, conjugate gradient search, steepest descent, simplex or Rosenbrock methods, simulated annealing, and genetic algorithm. The entire area of interest is partitioned into a finite grid, which is sequentially refined while looking for an optimal location. None of these methods guarantee a globally-optimal solution due to their intrinsic limitations or due to the non-convexity of underlying optimization problem. In addition, the cost function (the weighted sum pathloss) is introduced in an ad-hoc manner, without any link to system-level performance indicators (e.g. total transmit power or energy efficiency subject to QoS constraints).

B. UNMANNED AERIAL VEHICLES (UAV)

There is currently a growing interest in utilizing unmanned aerial vehicles (UAVs) as flying base stations to temporarily increase network capacity or/and provide coverage by moving supply towards demand [15], [16]. An algorithm to find a placement of UAV-BS that maximizes the number of covered users is proposed in [17]. The problem is decoupled into vertical and horizontal dimensions. For the vertical dimension, the optimum angle that maximizes the coverage radius and then the optimum height are found; in the horizontal dimension, the deployment is modeled as a circle placement problem. Further extending the above studies, a combination of terrestrial BSs with UAVs to improve the terrestrial network performance is considered in [18], [19], and [20] and iterative algorithms to determine optimal UAVs locations are proposed.

Optimal deployment of multiple UAVs with directional antennas serving randomly-located users via an orthogonal multiple-access scheme is considered in [22]. While the general case remains an open (NP-hard) problem, a closed-form asymptotic (in the number of UAVs) solution is obtained for uniformly-distributed users and all UAVs located at the same height. Based on numerical evidence, it is conjectured that the same height is asymptotically optimal in this case. Optimal deployment of tethered UAVs (T-UAV) to maximize cellular coverage and energy efficiency tradeoff in clusters of uniformly-distributed users is considered in [23], [28] using stochastic geometry tools and the SNR of a given user or the average pathloss as performance metrics. A set of locations to which optimal T-UAV location belongs is identified, and, since the remaining problems are analytically untractable, simulated annealing or exhaustive search are used. Intermittently tethered UAVs (iTUAVS) are proposed in [27] as a trade-off solution to combine the advantages of untethered and tethered UAVs. Optimal UAV placement is formulated in [24] as a constrained optimization problem to maximize fair coverage to energy consumption ratio while satisfying backhaul constraints. An algorithm for alternating optimization based on stochastic gradient decent is proposed and its performance is demonstrated via simulations. An algorithm to minimize the average UAV-user distance while maintaining UAV-terrestrial BS connectivity in LOS environment is presented in [26] and its convergence to a local optimum is proved. However, it is not clear how the average UAV-user distance relates to e.g. energy or spectral efficiencies, i.e. does the minimum average distance implies that the total transmit power is also minimized? Deployment and trajectory design of UAVs in non-orthogonal multiple-access (NOMA) wireless networks to maximise the network sum-rate are considered in [25]. Since the underlying optimization problems are non-convex and untractable analytically, balanced grey wolf optimization algorithm is used in combination with k-means clustering. A comprehensive model for the optimization of resource allocation and placement of UAVs in multi-hop (relaying) networks is proposed in [29]. While the model accounts for many relevant factors, it also renders the considered optimization problems untractable analytically and, due to their non-convexity, numerically as well, so that various approximations and bounds have to be used.

To summarize, while the above UAV deployment algorithms are useful from a practical perspective, they share the same fundamental limitations as those of the terrestrial BS location: since the underlying optimization problems are not convex and untractable analytically, convergence to global optima remains out of reach and the corresponding global optimality gap of the numerical solutions remains unknown. Therefore, it is not known whether the obtained solutions are close to the respective global optima or significant further improvement is still possible.

C. WIRELESS SENSOR NETWORKS

A related problem is that of optimal access point locations in wireless sensor networks (WSN), which have been studied extensively [30], [31], [32], [33], [34]. It should be noted, however, that there is a significant difference between optimal BS locations in cellular networks and those in wireless sensor networks, due to different operating conditions, system requirements and end-user demands. Indeed, while current cellular users demand high-rate services (e.g. streaming HD video as in 5G systems) and hence need high spectral efficiency in a limited bandwidth available (and often operate in interference-limited environment due to frequency re-use) [1], [35], autonomous sensors are low-rate energy-limited devices; their transmit power is much smaller than that of cellular users, and their batteries cannot be recharged on a regular basis, unlike those of cellular users. Hence, an optimal BS (access point, sink or cluster head) location in WSN is selected to maximize energy efficiency of autonomous sensors and hence prolong the network life time [30], [31], [32], [33], [34], while in cellular networks, BS location is selected to provide high rate (high spectral efficiency) to most cellular users and to minimize the amount of interference it creates (due to frequency re-use) to other cells [1], [35]. Since the same cellular BS serves many high-rate users at the same time in interference-dominated environment, its total transmit power is also of concern, unlike that in a sensor network. Thus, a BS location optimal for a cellular network is not necessarily optimal for a sensor network and vice versa.

D. COMMON LIMITATIONS

To summarize, while all the above-discussed algorithms are useful from the practical perspective, they have a number of limitations at the fundamental level. Due to the non-convex formulations or approximations they use, these algorithms converge to a *local optimum* at best, which can be far away from a *global optimum*; provable convergence to a global optimum is out of reach and the global optimality gap is not known (or bounded) either. If these algorithms are used to search for globally-optimal solutions (using e.g. multi-start implementation), they require exponentially-high complexity/run time (i.e., NP-hard) so that only small-sized problems can be handled in a reasonable time. This is a general difficulty for most non-convex problems [36], [37], [38]. Due to the numerical nature of the above algorithms, very limited or no insights are available. No closed-form solutions to the considered problems are known either. From a fundamental perspective, what is missing is an analytical framework for *globally*-optimal analysis, solutions and optimization algorithms.

E. OUR CONTRIBUTIONS

The aim of this paper is to build such a framework. To address the above gaps and limitations, the BS location problem is formulated here as a convex optimization problem to minimize the total BS transmit power subject to per-user rate constraints (other constraints can be added as well). Unlike the above-reviewed studies, this convex formulation delivers a *provable global optimum* efficiently, since its KKT conditions are sufficient for global optimality and numerical algorithms based on them, e.g. Newton barrier method, converge to a *global* (rather than local) optimum in polynomial time and run fast in practice, even for large problem instances (many users and constraints). In addition, a number of globally-optimum closed-form solutions, which cannot be found in the existing literature, are also presented here.

The system model is introduced in Section II, where a base station serves a given number of users with known locations and rate requirements. This may represent actual users in a cellular system as well as expected user distributions (e.g. in business or apartment buildings, shopping centers and other social attractors); expected traffic demands in different locations can also be represented in this way via virtual users [20], [21]. This system model is consistent with the current literature on optimal BS location [5], [6], [7], [8], [9], [10], [12], [13], [14], [16], [17], [18], [19], [20], [21], [22], [23], [24], [25], [26], [27], [28], [29], [30], [31], [32], [33], [34]. While we consider first a single base station scenario, the obtained results can be used as a building block to solve higher-level problems with multiple base stations (an approach used extensively in the current literature), as demonstrated in Section VII. The considered model and approach are general enough to include any rate that is a monotonically-increasing function of the SNR and hence can include fading, in addition to the average pathloss, as well as nonuniform user (traffic) distributions. It is also applicable to modern systems using massive MIMO and millimeter waves (key technologies for 5G/6G systems), which rely on orthogonal access schemes in frequency, time or space domains [35]. Different propagation conditions to different users are accommodated as well. In particular, unobstructed line-of-sight (LOS) propagation (where 1st Fresnel zone is clear of any obstructions) corresponds path loss exponent $\nu = 2$ while obstructed LOS corresponds to $2 < \nu < 8$, where higher ν represents heavier obstruction; $\nu < 2$ is also possible in waveguide-type environments, e.g., tunnels, corridors, shopping malls/warehouses etc. [45], [46], [47], [48], [63], [64].

Next, the optimal BS location problem is formulated as a convex optimization problem to minimize the total BS transmit power, subject to the QoS (per-user rate) constraints; additional constraints are also considered later on. Based on this novel formulation, Section III characterizes a *globally-optimal* BS location in the general 3-D case as a convex combination of user locations, where the convex weights depend on user bandwidth and rate demands, some system and propagation parameters, and overall geometry of the problem.

This characterization is subsequently used to obtain a number of explicit closed-form solutions for an optimal BS location (to the best of our knowledge, for the first time). In the case of users with identical parameters (rate and bandwidth) and line-of-sight propagation ($\nu = 2$), the globally-optimal BS location is shown to be the average (arithmetic mean) of user locations. This also applies to other propagation environments provided that the set of users is symmetric (as defined in the paper), or to randomly-located users, where the optimal BS location converges to the mean user location as the number of users increases. In the case of a symmetric set of users, the optimal BS location is also independent of pathloss exponent ν while the latter has a profound impact on the optimal BS location for asymmetric user sets. In the case of heavily obstructed LOS and hence large pathloss exponent ($\nu > 4$), the optimal BS location is determined by the most distant user locations. In general, users with higher rate demands are shown to contribute more to an optimal BS location (via their convex weights) and distant users have higher weights for larger ν (i.e. for heavier LOS obstruction).

Clustered environments are also considered, where all users are grouped into several clusters, and an optimal BS location is shown to be the average of cluster centers provided that the inter-cluster distances are significantly larger than the cluster sizes. An unusual property is observed whereby an optimal BS location is not necessarily unique. While the optimal BS location is always unique when the pathloss exponent $\nu > 1$, this is not necessarily the case with $\nu = 1$ (this may represent some waveguide-type environments), as shown for collinear users in Section III-F. However, it is always unique for the elevated BS case.

While the study above considers the general 3-D user locations, Section IV considers an elevated BS scenario, where all users are located on a 2-D (ground) plane and the BS is elevated above it. This may represent typical BS locations in cellular systems as well as UAV-based base stations. The optimal BS location is characterized as a convex combination of user locations, where the weights depend on user parameters and pathloss exponent, subsequently elevated above the ground plane.

Section V extends the original problem to include extra constraints on a BS location (where the BS must be located within a certain available area, e.g. a rooftop or a hill). The characterization of Section III as well as many other results are shown to hold for this extended problem as well.

Section VI presents an iterative algorithm for the BS location problem for the general case (unequal system/user parameters and pathloss exponents) and its convergence is established in Proposition 7. For the $\nu = 1$ case, this Algorithm reduces to the Weiszfeld's Method [71], [72], [73] to solve the celebrated 350-years-old Fermat-Weber problem [71], but is substantially different from it in other cases.

The single-BS results above are extended to a multi-BS setting (a cell cluster) in Sec. VII. Since the total (sum) BS power minimization for the entire cellular cluster (via proper user-BS assignment and BS location) is a non-convex problem, we show that the popular K-means algorithm can be used (with proper modifications) to find a locally-optimal solution to this problem. Unlike the known studies making use of this algorithm [52], [53], [54], [55], [56], [57], [58], [59], we use the physically-based "distance" measure to make sure that the total BS power is reduced at each iteration of the algorithm. Consequently, an algorithm convergence point corresponds to a locally-optimal BS locations that minimize the total power of all base stations in the cellular cluster. A globally-optimal location can be approached by using the multi-start version of the algorithm. Its computational complexity can be reduced by using the above analytical location results at each iteration.

To facilitate the analysis and to obtain insights, we consider the users having the same path loss exponent and other system parameters in some parts of the paper. However, our approach is not limited to this setting: different path loss exponents and system parameters can be accommodated as well, as in Theorems 1-3, Propositions 2, 3, 7 and in Section VI and VII, including Algorithms 1 and 2.

Representative numerical experiments are considered in Section VIII, which validate the analytical results and related approximations and show the effectiveness of the proposed algorithms.

Overall, this paper studies analytically an optimum BS location to minimize its total transmit power (subject to per-user rate constraints) as well as the impact of pathloss exponent, system parameters and traffic (user) distribution. Its analytical results provide insights unavailable from numerical algorithms/studies and can be subsequently used to obtain design guidelines for more complicated settings. Compared to the known studies and algorithms, *globally* (rather than locally)-optimal solutions are obtained here in an efficient way, sometimes in a closed-form.

II. SYSTEM MODEL AND PROBLEM FORMULATION

Following the approach widely accepted in the current literature [5], [6], [7], [8], [9], [10], [12], [13], [14], [16], [17], [18], [19], [20], [21], [22], [23], [24], [25], [26], [27], [28], [29], [30], [31], [32], [33], [34], let us consider a base station (BS) serving N users located at $\boldsymbol{x}_n$, $n = 1, .., N$, via some form of an orthogonal multiple-access technique, e.g. frequency-division multiple access (FDMA), time-division multiple access (TDMA) or space-division multiple access (SDMA), which are widely used by modern systems [35]. Due to spatial filtering using a large number of antennas and the phenomenon known as "favorable propagation", user orthogonality is also ensured in massive MIMO multi-user systems [60], [61], [62]. Large bandwidth available to millimeter-wave systems (a key technology for 5G/6G systems) also makes an orthogonal access the preferred choice [63], [64]. Under this assumption, user rates R_n can be expressed as follows,

$$R_n = \Delta f_n \log(1 + \gamma_n/\Gamma_n) \tag{1}$$

where Δf_n and $\gamma_n = P_{rn}/\sigma_{0n}^2$ are the bandwidth and the SNR of user n, the channel is frequency-flat with AWGN noise of power σ_{0n}^2 and P_{rn} is the signal power received by user n; $\Gamma_n \geq 1$ is the SNR gap to the capacity of user n [40], [41], [42], [43] (it can also represent "interference margin" and model the residual inter-user interference from co-channel cells). When efficient (capacity-approaching) codes are used for each user, $\Gamma_n \rightarrow 1$. In practice, the assumption of rates being close to the capacity is justified due to the existence of codes which operate very close to channel capacity, e.g. turbo, polar or LDPC codes [44]. In fact, this model can be further extended to include any rate which is a monotonically-increasing function of the SNR (e.g. an ergodic rate in a fading channel) by properly selecting β_n in (4). While we do not consider inter-user interference (due to e.g. frequency re-use) explicitly, the solutions we obtain will minimize the total Tx power for each BS and therefore the amount of inter-user interference will also be minimized. In addition, the use of massive or ultra-massive MIMO in 5G/6G systems effectively eliminates inter-user interference via spacial filtering under the condition known as "favorable propagation" [60], [61], [62] and modern millimeter-wave systems are known to be noise-dominated (due to large bandwidth available and large path loss to distant users) [63], [64]. Hence, our approach is applicable to such systems as well.

The received power P_{rn} is related to the transmit power P_n allocated by the BS to user n via the path loss model [45], [46], [47], [48],

$$P_{rn} = \alpha_n P_n / d_n^{\nu_n} \tag{2}$$

where $d_n = |\boldsymbol{c} - \boldsymbol{x}_n|$ is the distance between the BS located at $\boldsymbol{c}$ and user n located at $\boldsymbol{x}_n$, $|\boldsymbol{x}|$ is the Euclidean norm (length) of vector $\boldsymbol{x}$, ν_n is the path loss exponent, and α_n is a constant related to the propagation environment and antenna gains (due to e.g. beamforming), which is independent of distance but may depend on frequency. For example, in the case of free-space propagation environment in the far-field, e.g. when line-of-sight (LOS) path is dominant, $\nu_n = 2$ and $\alpha_n = G_{tn}G_{rn}(\lambda_n/(4\pi))^2$, where λ_n is the wavelength of user n and G_{tn}, G_{rn} are the Tx and Rx antenna gains. For the 2-ray ground reflection model, $\nu_n = 4$ and $\alpha_n = G_{tn}G_{rn}h_t^2 h_{rn}^2$, where h_t, h_{rn} are the transmit (BS) and user n antenna heights [45]. LOS blockage can be accounted for via larger ν_n: the larger the blockage, the larger the path loss exponent is: while $\nu_n = 2$ corresponds to clear LOS (unobstructed 1ts Fresnel zone), $\nu_n = 2.5 \ldots 8$ correspond to lightly to severely blocked LOS, and $\nu_n < 2$ corresponds to waveguide-type environments with clear LOS [45]. The model in (2) is widely used in the literature [5], [6], [7], [8], [9], [10], [12], [13], [14], [16], [17], [18], [19], [20], [21], [22], [23], [24], [25], [26], [27], [28], [29], [30], [31], [32], [33], [34] as well as in the current industrial standards [46]. It has been extensively tested experimentally [45], [46], [47], [48], [63], making it practically-relevant.

Since a cellular BS location is fixed and cannot be changed every time a user experiences a different fading state or moves around, only the average path loss is included in (2) to represent long-term tendencies (it is understood that the system performance for a particular user in a given moment of time may depend on its channel fading state at that time). However, the impact of fading can be included by considering an ergodic rate function instead of (1), which also corresponds to (4) with a properly selected β_n so that all our results apply to an ergodic fading scenario as well. Modern systems using massive MIMO effectively eliminate small-scale fading due to the effect known as "channel hardening" [60] (roughly, this corresponds to high-order diversity combining using a large number of antennas). Hence, our approach is applicable to such systems as well.

We assume that the BS knows path loss to each user (or, equivalently, its SNR). While there may be significant short-term user dynamics in terms of locations, rate demands, fading, etc. in real-world systems, our model is not intended to model this dynamics but rather to represent long-term tendencies in user locations and service demands since we consider a fixed (rather than mobile) BS. While scheduling/resource allocation algorithms take care of this short-term dynamics in real time, a fixed BS location is selected based on long-term tendencies in user locations and service demands and this location is not expected to change following short-term dynamics (unless one considers a UAV BS). Therefore, only the average path loss is taken into account in (2). To satisfy quality-of-service requirements, each user rate must not be less than its target rate R_{0n}: $R_n \geq R_{0n}$, where the latter is determined based on user's grade of service and traffic/service demand (adaptive modulation/coding along with time/frequency resource blocks are used practice to set it up [35]). To achieve this objective in an energy-efficient way, the operator selects BS location $\boldsymbol{c}$ in an optimal way to minimize its total transmit power $P_T = \sum_n P_n$ subject to the QoS constraints as follows:

$$\text{(P1)} \ \min_{\{P_n\},\boldsymbol{c}} \sum_n P_n \ \text{ s.t. } \ R_n \geq R_{0n} \tag{3}$$

where the optimization variables are BS location $\boldsymbol{c}$ as well as per-user powers $\{P_n\}$, so that the BS performs optimal per-user power allocation as well. Noting from (1) that the constraint $R_n \geq R_{0n}$ is equivalent to $\gamma_n \geq \gamma_{0n} = (2^{R_{0n}/\Delta f_n} - 1)\Gamma_n$, the problem (P1) can be re-formulated as follows:

$$\text{(P2)} \ \min_{\{P_n\},\boldsymbol{c}} \sum_n P_n \ \text{ s.t. } \ P_n \geq \beta_n |\boldsymbol{c} - \boldsymbol{x}_n|^{\nu_n} \tag{4}$$

where β_n absorbs all system-level parameters,

$$\beta_n = \frac{\gamma_{0n}\sigma_{0n}^2}{\alpha_n} = \frac{(2^{R_{0n}/\Delta f_n} - 1)\Gamma_n \sigma_{0n}^2}{\alpha_n} \tag{5}$$

Note that σ_{0n}^2 may also include interference power as a part of it. We further note that problem (P1) and hence (P2) can also accommodate any rate model that is a monotonically-increasing function of the SNR $R_n(\gamma_n)$, not only that in (1), so that the condition $R_n \geq R_{0n}$ is equivalent to $\gamma_n \geq \gamma_{0n}$ with properly-selected $\gamma_{0n} = R_n^{-1}(R_{0n})$. This generalized model can also include fading, where R_n and γ_n are interpreted as the average (ergodic) rate and SNR respectively.

To the best of our knowledge, no analytical solution is available in the literature to either (P1) or (P2). Therefore, the next section presents a general characterization of an optimal BS location according to (P2), from which a number of closed-form solutions are obtained in some special cases. These results are further extended to multi-BS location problem in Section VI. Unless indicated otherwise, "optimal" means "globally-optimal" in the rest of this paper.

III. OPTIMAL BS LOCATION AND POWER ALLOCATION

Following the model of the previous section, a globally-optimal BS location and power allocation to minimize the total transmit power subject to the QoS constraints can be characterized as follows.

Theorem 1: A globally-optimal BS location $\boldsymbol{c}^*$ in (4) can be expressed as a convex combination of user locations $\{\boldsymbol{x}_n\}$:

$$\boldsymbol{c}^* = \sum_n \theta_n \boldsymbol{x}_n, \ \theta_n = \frac{\beta_n \nu_n |\boldsymbol{c}^* - \boldsymbol{x}_n|^{\nu_n - 2}}{\sum_n \beta_n \nu_n |\boldsymbol{c}^* - \boldsymbol{x}_n|^{\nu_n - 2}} \tag{6}$$

if either (i) $\nu_n \geq 2$ or/and (ii) $\boldsymbol{c}^* \neq \boldsymbol{x}_n$ and $\nu_n \geq 1$, where $0 \leq \theta_n \leq 1$, $\sum_n \theta_n = 1$. Transmission with the least per-user power is optimal: $P_n^* = \beta_n |\boldsymbol{c}^* - \boldsymbol{x}_n|^{\nu_n}$.

Proof: Since the problem (P2) in (4) is convex and the strong duality holds (Slater condition is satisfied), its KKT conditions are sufficient for optimality [36]. Its Lagrangian is

$$L(P_n, \boldsymbol{c}) = \sum_n P_n + \sum_n \lambda_n (\beta_n |\boldsymbol{c} - \boldsymbol{x}_n|^{\nu_n} - P_n) \tag{7}$$

where $\lambda_n \geq 0$ are Lagrange multipliers responsible for the power constraints. First, we consider the non-singular case, when $\boldsymbol{c}^* \neq \boldsymbol{x}_n \ \forall n$, and deal with the singular case later on. In the non-singular case, the KKT conditions take the following form

$$\frac{\partial L}{\partial \boldsymbol{c}} = \sum_n \lambda_n \beta_n \nu_n (\boldsymbol{c} - \boldsymbol{x}_n)|\boldsymbol{c} - \boldsymbol{x}_n|^{\nu_n - 2} = 0, \tag{8}$$

$$\frac{\partial L}{\partial P_n} = 1 - \lambda_n = 0 \tag{9}$$

$$\lambda_n (\beta_n |\boldsymbol{c} - \boldsymbol{x}_n|^{\nu_n} - P_n) = 0 \tag{10}$$

$$P_n \geq \beta_n |\boldsymbol{c} - \boldsymbol{x}_n|^{\nu_n}, \ \lambda_n \geq 0 \tag{11}$$

where (8), (9) are the stationary conditions, (10) are the complementary slackness conditions, and (11) are primal and dual feasibility conditions. 1st condition in (8) was obtained from

$$\frac{\partial |\boldsymbol{x}|^\nu}{\partial \boldsymbol{x}} = \nu \boldsymbol{x} |\boldsymbol{x}|^{\nu - 2} \tag{12}$$

if $\boldsymbol{x} \neq 0$, which always holds in the non-singular case. The 2nd condition in (8) implies $\lambda_n = 1$ so that, from (10), $P_n = \beta_n |\boldsymbol{c} - \boldsymbol{x}_n|^{\nu_n}$, i.e. transmitting with the least required power for each user is optimal. Combining this with 1st condition in (8) results, after some manipulations, in (6).

The singular case, when $\boldsymbol{c}^* = \boldsymbol{x}_n$ for some n, is more involved as, in this case, (12) and hence 1st condition in (8) do not hold (since $\boldsymbol{x} = 0$ and $|\boldsymbol{x}|$ is not differentiable at $\boldsymbol{x} = 0$). To deal with this case, we consider a regularized version of (P2) of the following form:

$$\min_{P_n, \boldsymbol{c}} \sum_n P_n \ \text{ s.t. } P_n \geq \beta_n |\boldsymbol{c} - \boldsymbol{x}_n|_h^{\nu_n} \tag{13}$$

where $|\boldsymbol{x}|_h = (|\boldsymbol{x}|^2 + h^2)^{1/2}$, for some $h \neq 0$. Since $|\boldsymbol{x}|_h$ is differentiable for any $\boldsymbol{x}$ (including $\boldsymbol{x} = 0$) when $h \neq 0$, the singularity is always avoided and one can use the same KKT-based approach as above. The respective KKT conditions are:

$$\frac{\partial L}{\partial \boldsymbol{c}} = \sum_n \lambda_n \beta_n \nu_n (\boldsymbol{c} - \boldsymbol{x}_n)|\boldsymbol{c} - \boldsymbol{x}_n|_h^{\nu_n - 2} = 0, \quad (14)$$

$$\frac{\partial L}{\partial P_n} = 1 - \lambda_n = 0 \quad (15)$$

$$\lambda_n(\beta_n |\boldsymbol{c} - \boldsymbol{x}_n|_h^{\nu_n} - P_n) = 0 \quad (16)$$

$$P_n \geq \beta_n |\boldsymbol{c} - \boldsymbol{x}_n|_h^{\nu_n}, \ \lambda_n \geq 0 \quad (17)$$

where we have used

$$\frac{\partial |\boldsymbol{x}|_h^{\nu}}{\partial \boldsymbol{x}} = \nu \boldsymbol{x} |\boldsymbol{x}|_h^{\nu - 2} \quad (18)$$

valid for any $\boldsymbol{x}$, including $\boldsymbol{x} = 0$, hence avoiding the singularity problem. Solving the KKT conditions in the same way as above, one obtains the optimal location $\boldsymbol{c}^*(h)$ as follows:

$$\boldsymbol{c}^*(h) = \sum_n \theta_n(h) \boldsymbol{x}_n, \quad (19)$$

$$\theta_n(h) = \frac{\beta_n \nu_n |\boldsymbol{c}^*(h) - \boldsymbol{x}_n|_h^{\nu_n - 2}}{\sum_n \beta_n \nu_n |\boldsymbol{c}^*(h) - \boldsymbol{x}_n|_h^{\nu_n - 2}} \quad (20)$$

To proceed further, let $P_T = \sum_n \beta_n |\boldsymbol{c}^* - \boldsymbol{x}_n|^{\nu_n}$ and $P_h = \sum_n \beta_n |\boldsymbol{c}^*(h) - \boldsymbol{x}_n|_h^{\nu_n}$ be the optimal total transmit powers of the BS for the original and regularized problems, and $P_T(\boldsymbol{c}) = \sum_n \beta_n |\boldsymbol{c} - \boldsymbol{x}_n|^{\nu_n}$ be the total BS transmit power for the original problem when the BS is located at $\boldsymbol{c}$ (not necessarily optimal). Their relationship can be characterized as follows.

Lemma 1: The powers P_T, $P_T(\boldsymbol{c})$ and P_h are related as follows:

$$P_T \leq P_T(\boldsymbol{c}^*(h)) \leq P_h \quad (21)$$

where $P_T(\boldsymbol{c}^*(h))$ is the total BS power of the original problem when it is located at $\boldsymbol{c}^*(h)$, i.e. the optimal location of the regularized problem. Furthermore,

$$\lim_{h \to 0} P_h = P_T = \lim_{h \to 0} P_T(\boldsymbol{c}^*(h)) \quad (22)$$

and, when the limit exists, $\lim_{h \to 0} \boldsymbol{c}^*(h) = \boldsymbol{c}^*$.

Proof: Since

$$|\boldsymbol{c} - \boldsymbol{x}_n|^{\nu_n} \leq |\boldsymbol{c} - \boldsymbol{x}_n|_h^{\nu_n} \quad (23)$$

for any $\boldsymbol{c}$, k and h, it follows that

$$P_h = \sum_n \beta_n |\boldsymbol{c}^*(h) - \boldsymbol{x}_n|_h^{\nu_n} \quad (24)$$

$$\geq P_T(\boldsymbol{c}^*(h)) \geq \min_{\boldsymbol{c}} P_T(\boldsymbol{c}) = P_T \quad (25)$$

as required. Since $|\boldsymbol{c} - \boldsymbol{x}_n|_h^{\nu_n}$ is continuous and

$$\lim_{h \to 0} |\boldsymbol{c} - \boldsymbol{x}_n|_h^{\nu_n} = |\boldsymbol{c} - \boldsymbol{x}_n|^{\nu_n} \quad (26)$$

it follows that $\lim_{h \to 0} P_h = P_T$ and hence, from (24),

$$\lim_{h \to 0} P_T(\boldsymbol{c}^*(h)) = P_T \quad (27)$$

and, when the limit exists,

$$\lim_{h \to 0} \boldsymbol{c}^*(h) = \boldsymbol{c}^* \quad (28)$$

since $P_T(\boldsymbol{c})$ is a continuous function. □

Now notice that the KKT conditions (14)-(17) of the regularized problem converge to those of the original problem in (8)-(11) if $\nu_n \geq 2$, since $|\boldsymbol{x}|_h \to |\boldsymbol{x}|$ as $h \to 0$ and the regularized KKT conditions are continuous in h when $\nu_n \geq 2$ (even if $\boldsymbol{c} = \boldsymbol{x}_n$). Hence, $\boldsymbol{c}^*(h) \to \boldsymbol{c}^*$ as $h \to 0$, i.e. the regularized problem solution converges to that of the original one and thus (6) holds in full generality when $\nu_n \geq 2$ (even in the singular case $\boldsymbol{c}^* = \boldsymbol{x}_n$). This concludes the proof of Theorem 1. □

Next, we explore some properties of an optimal BS location to get some insight in the general case.

Proposition 1: When $\nu_n > 1$ for some n, an optimal base station location is unique. This is not necessarily the case if $\nu_n = 1$ for all n.

Proof: We need the following technical lemma.

Lemma 2: The function $f(\boldsymbol{x}) = |\boldsymbol{x}|^{\nu}$ is strictly convex for any $\nu > 1$.

Proof: For any $\boldsymbol{x}, \boldsymbol{y}$, $0 \leq \theta \leq 1$, the following holds:

$$\begin{aligned} f(\theta \boldsymbol{x} + (1-\theta)\boldsymbol{y}) &= |\theta \boldsymbol{x} + (1-\theta)\boldsymbol{y}|^{\nu} \\ &\leq (\theta |\boldsymbol{x}| + (1-\theta)|\boldsymbol{y}|)^{\nu} \\ &\leq \theta |\boldsymbol{x}|^{\nu} + (1-\theta)|\boldsymbol{y}|^{\nu} \\ &= \theta f(\boldsymbol{x}) + (1-\theta) f(\boldsymbol{y}) \end{aligned} \quad (29)$$

where 1st inequality is due to the triangle inequality,

$$|\theta \boldsymbol{x} + (1-\theta)\boldsymbol{y}| \leq \theta |\boldsymbol{x}| + (1-\theta)|\boldsymbol{y}| \quad (30)$$

and the fact that x^{ν} is strictly increasing, while 2nd inequality is due to the convexity of x^{ν} for $\nu > 1$. To establish strict convexity, let $\boldsymbol{x} \neq \boldsymbol{y}$ and $0 < \theta < 1$, and observe that 1st inequality in (29) is strict if $\boldsymbol{x} \neq \alpha \boldsymbol{y}$ for any $\alpha > 0$, due to the strict inequality in (30) in this case, and hence

$$f(\theta \boldsymbol{x} + (1-\theta)\boldsymbol{y}) < \theta f(\boldsymbol{x}) + (1-\theta) f(\boldsymbol{y}) \quad (31)$$

as required. On the other hand, if $\boldsymbol{x} = \alpha \boldsymbol{y}$ for some $\alpha > 0$, $\alpha \neq 1$, then $|\boldsymbol{x}| \neq |\boldsymbol{y}|$ and 2nd inequality in (29) is strict, due to the strict convexity of x^{ν} for $\nu > 1$, hence implying (31). □

Now, the uniqueness of the solution follows from the fact that (P2) is equivalent to

$$\min_{\boldsymbol{c}} \sum_n \beta_n |\boldsymbol{c} - \boldsymbol{x}_n|^{\nu_n} \quad (32)$$

since transmitting with the least per-user power is optimal, and the objective here is strictly convex if $\nu_n > 1$ for some k, from Lemma 2, and thus the solution is unique [36]. Non-uniqueness for $\nu_n = 1$ can be shown via examples, see Proposition 5 and Fig. 7. This concludes the proof of Proposition 1.

To proceed further, we need the following definition [36].

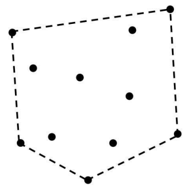

FIGURE 1. The convex hull of a set of points (shown as dots) in $\mathbb{R}^2$ is a pentagon (with dashed boundary).

Definition 1: Let $\{\boldsymbol{y}_n\}$ be a set of points. Its convex hull $\mathbf{conv}\{\boldsymbol{y}_n\}$ *is the set of all convex combinations of the points in $\{\boldsymbol{y}_n\}$:*

$$\mathbf{conv}\{\boldsymbol{y}_n\} = \left\{ \sum_n q_n \boldsymbol{y}_n : q_n \geq 0, \sum_n q_n = 1 \right\} \tag{33}$$

Figure 1 illustrates this definition. Note that $\mathbf{conv}\{\boldsymbol{y}_n\}$ is always a convex set, regardless of $\{\boldsymbol{y}_n\}$.

Corollary 1: The optimal BS location $\boldsymbol{c}^*$ in (6) is in the convex hull of all user locations:

$$\boldsymbol{c}^* \in \mathbf{conv}\{\boldsymbol{x}_n\} \tag{34}$$

Proof: Notice from (6) that $0 \leq \theta_n \leq 1$, $\sum_n \theta_n = 1$, and then apply Definition 1. □

While (6) characterizes an optimal location of the BS, no closed-form solution of this relationship is known in the general case (note that (6) is not a closed-form solution itself since θ_n depends on $\boldsymbol{c}^*$). The above Corollary gives a property of such solution. Furthermore, it implies that the search of $\boldsymbol{c}^*$ can always be confined to $\mathbf{conv}\{\boldsymbol{x}_n\}$, without loss of optimality. For example, if all users are located on a line or in a building, the optimal BS is also on this line or in this building.

We obtain below a number of explicit closed-form solutions for $\boldsymbol{c}^*$ in some special but practically-important cases.

A. LINE-OF-SIGHT PROPAGATION

An important special case, included in industrial standards, is that of LOS or free-space propagation, where $\nu_n = 2$. In practice, $\nu_n \approx 2$ when most of the 1st Fresenel zone is free of obstructions [45], [46], [47], [48]. This is also the case in a multipath channel when multipath components are much weaker than LOS; therefore, LOS dominates and the propagation becomes almost the same as in free space. ν_n is close to 2 in many indoor environments when LOS is present [45] and $\nu_n = 2$ appears often in the industrial propagation models [46]. This propagation environment is also critical for emerging millimeter wave (mmWave) or THz systems (key technologies for 5/6G), where any significant blockage of LOS results in link outage due to high propagation path loss and therefore low SNR [63], [64], [65], [66].

Using Theorem 1, the optimal BS location $\boldsymbol{c}^*$ can be expressed as follows in this environment.

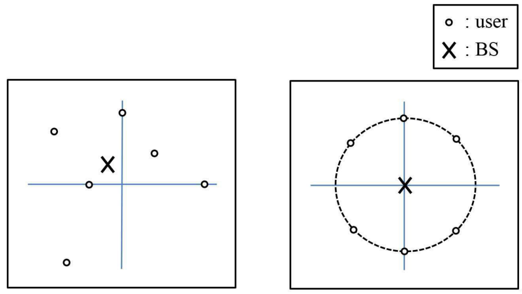

FIGURE 2. Left: an irregular user set and optimum BS location. Right: an equivalent symmetric set of users, which requires the same BS power and the users get the same rates as on the left.

Corollary 2: If $\nu_n = 2$ for all n, the optimal BS location $\boldsymbol{c}^*$ is a weighted average of the user locations:

$$\boldsymbol{c}^* = \sum_n \theta_n \boldsymbol{x}_n, \ \theta_n = \frac{\beta_n}{\sum_i \beta_i}. \tag{35}$$

where $0 \leq \theta_n \leq 1$, $\sum_n \theta_n = 1$.

Proof: Use (6) with $\nu_n = 2$. □

Note that (35) is an explicit closed-form solution, since θ_n are now independent of $\boldsymbol{c}^*$. It follows that users with larger β_n, i.e. those requiring higher rates, contribute more to $\boldsymbol{c}^*$ so that as β_n increases, $\boldsymbol{c}^*$ moves closer to $\boldsymbol{x}_n$. In the limiting case of $\beta_1 > 0, \ \beta_i = 0, i \neq 1$, the optimal location $\boldsymbol{c}^* = \boldsymbol{x}_1$.

Further simplification is possible when all users require the same rate and have the same system settings, so that $\beta_n = \beta \ \forall n$.

Corollary 3: If $\nu_n = 2$ and $\beta_n = \beta \ \forall n$, the optimal BS location $\boldsymbol{c}^*$ is the average of user locations:

$$\boldsymbol{c}^* = \bar{\boldsymbol{x}} = \frac{1}{N} \sum_n \boldsymbol{x}_n. \tag{36}$$

The total BS transmit power $P_T = \sum_n P_n$ is proportional to the empirical variance σ^2 of user locations,

$$P_T = N\beta\sigma^2, \tag{37}$$

where $\sigma^2 = N^{-1} \sum_n |\bar{\boldsymbol{x}} - \boldsymbol{x}_n|^2$.

Proof Use (35) with $\beta_n = \beta$. (37) follows from (36). □

Note that (37) also represents the total BS power when all N users are located at the same distance σ from the BS, i.e. on a circle (or sphere) of radius σ centered on the BS, where $P = \beta\sigma^2$ represents per-user BS power. Hence, the original, possibly highly irregular, user setting can be equivalently substituted by a highly-symmetric (circular) user locations, keeping the same total BS power as well as the same total and per-user rates (however, the per-user powers are not necessarily the same). This is illustrated in Fig. 2.

B. RANDOMLY-LOCATED USERS

It should be pointed out that (35) and (36) can also used to find the optimal BS location for randomly-located users. Indeed, when $\boldsymbol{x}_n$ are independent identically-distributed (iid) random vectors of finite variance, the law of large numbers (LLN)

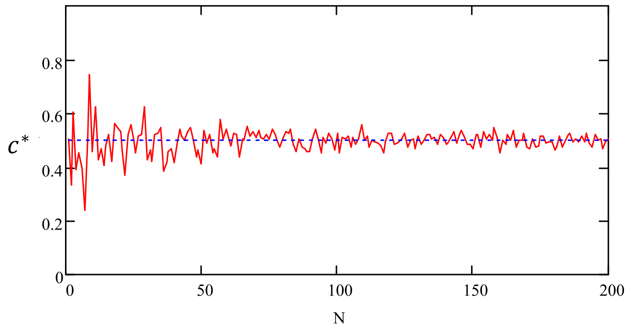

FIGURE 3. The optimal BS location c^* (solid red) and its statistical mean $\mathbb{E}\{c^*\} = \mathbb{E}\{x\} = 1/2$ (dashed blue) for N random users uniformly distributed on the unit line segment [0,1] (for each value of N, the set of all N user locations was generated afresh).

applies [67, p. 12] [68, p. 185] so that, using (35), $\boldsymbol{c}^*$ will converge to its statistical mean $\mathbb{E}\{\boldsymbol{c}^*\}$ as the number N of users increases:

$$\boldsymbol{c}^* \to \mathbb{E}\{\boldsymbol{c}^*\} = \sum_n \theta_n \mathbb{E}\{\boldsymbol{x}_n\} = \mathbb{E}\{\boldsymbol{x}\} \tag{38}$$

where $\mathbb{E}\{\boldsymbol{x}\} = \mathbb{E}\{\boldsymbol{x}_n\}$ is the statistical mean of user locations (all means are the same due to the iid assumption) and the convergence is in probability, mean-square error or with probability one. Thus, in this case, the globally-optimal BS location converges to the statistical mean of user locations and this also holds for the setting of Corollary 3.

To illustrate this stochastic convergence, let us consider an example where N independent users are uniformly distributed on the unit interval [0,1] (this can be a normalized distance along a line, e.g. a street) so that $\mathbb{E}\{\boldsymbol{x}\} = 1/2$. Fig. 3 shows the convergence of $\boldsymbol{c}^*$ to $\mathbb{E}\{\boldsymbol{c}^*\} = \mathbb{E}\{\boldsymbol{x}\} = 1/2$ as N increases, where an independent set of user locations was generated for each value of N to illustrate statistical fluctuations of $\boldsymbol{c}^*$, which quickly diminish as N increases. Clearly, $\boldsymbol{c}^* \approx \mathbb{E}\{\boldsymbol{x}\}$ is a good approximation for $N \geq 100$ so that using individual random locations $\boldsymbol{x}_n$ of users to optimize BS location does not bring in any significant advantage compared to using the mean user location $\mathbb{E}\{\boldsymbol{x}\}$ instead. This example also applies to a two-dimensional settings, where users are distributed on a unit square (where each coordinate is uniformly and independently distributed); in this case, Fig. 3 should be interpreted as representing one coordinate of the optimal BS location.

This result can also be extended to a more general setting where user locations are still independent but with different distributions of bounded variances and different statistical means $\mathbb{E}\{\boldsymbol{x}_n\}$. In this case,

$$\boldsymbol{c}^* \to \sum_n \theta_n \mathbb{E}\{\boldsymbol{x}_n\} \tag{39}$$

i.e. the globally-optimal BS location converges to the weighted average of statistical means of user locations. Likewise, when $\beta_n = \beta\ \forall n$ as in Corollary 3, this becomes just the average of statistical means,

$$\boldsymbol{c}^* \to \frac{1}{N} \sum_n \mathbb{E}\{\boldsymbol{x}_n\} \tag{40}$$

Finally, the case of correlated user locations can also be considered since the LLN is also applicable to some cases of correlated random variables (e.g. when Bernstein's conditions hold) [69], [70]. However, the analysis becomes significantly more complicated and is beyond the scope of this paper.

C. LARGE PATHLOSS EXPONENT

To obtain further insights, we return to deterministically-located users and consider the limiting case of large pathloss exponent $\nu_n \to \infty$, which serves as an approximation to large but finite ν_n (as will be seen from numerical experiments below). To simplify the discussion, we further assume that all users have identical parameters so that $\beta_n = \beta\ \forall n$.

Proposition 2: If $\nu_n \to \infty$, the optimal BS location is the average of most distant user locations.

Proof: Without loss of generality, arrange users according to their distances to the BS in a descending order, i.e. $d_1 = d_2 = \ldots = d_p > d_{p+1} \geq \ldots \geq d_N$, where p is the number of most distant users. Then, θ_i can be expressed as

$$\begin{aligned}\lim_{\nu_n \to \infty} \theta_i &= \lim_{\nu_n \to \infty} \frac{d_i^{\nu_n - 2}}{\sum_n d_n^{\nu_n - 2}} \\ &= \lim_{\nu_n \to \infty} \left(\sum_{n=1}^{p} \left(\frac{d_n}{d_i}\right)^{\nu_n - 2} + \sum_{n=p+1}^{N} \left(\frac{d_n}{d_i}\right)^{\nu_n - 2} \right)^{-1} \\ &= \begin{cases} p^{-1}, & 1 \leq i \leq p, \\ 0, & i > p, \end{cases}\end{aligned} \tag{41}$$

and therefore,

$$\boldsymbol{c}^* = \frac{1}{p} \sum_{n=1}^{p} \boldsymbol{x}_n \tag{42}$$

□

Hence, for large path loss exponent, it is the most distant users who determine the optimal BS location, while nearby users contribute little.[1] Finding most distant users in a set can be expressed geometrically as follows. First, generate a sphere large enough to enclose all the users. Then, shrink it until no further shrinkage is possible while keeping all the users inside, as illustrated in Fig. 4, thus obtaining the smallest enclosing sphere. The most distant users are those on the sphere surface. This can also be expressed as a convex optimization problem below, where optimization variables are the sphere center $\boldsymbol{c}$ and its radius r:

$$\min_{r,\boldsymbol{c}} r \text{ s.t.} |\boldsymbol{c} - \boldsymbol{x}_n| \leq r\ \forall n \tag{43}$$

[1] In real-world applications, BS transmit power to each user may be limited and, if the threshold is exceeded since the user is located far away ("outlier"), its power should be set to the maximum allowed level; alternatively, outliers may be excluded from the service or re-assigned to a different BS.

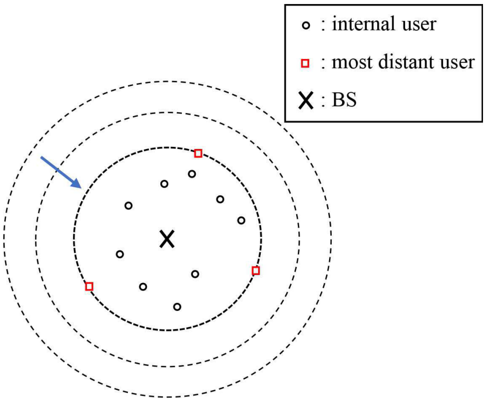

FIGURE 4. An illustration of finding the most distant users via enclosing spheres.

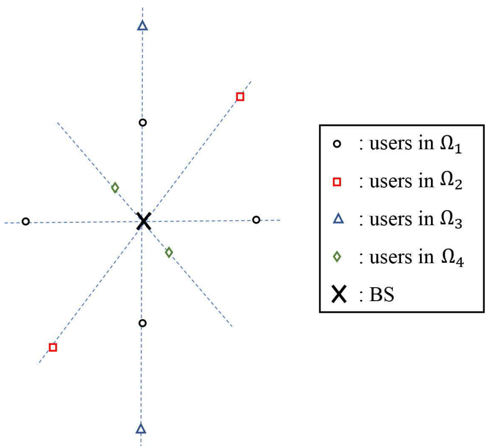

FIGURE 5. The union of 4 elementary symmetric sets $\Omega_1..\Omega_4$ with the same center is symmetric; the optimal BS location, for any pathloss exponent ν, is its (common) center.

D. SYMMETRIC SETS OF USERS

To obtain closed-form solutions for $\boldsymbol{c}^*$ beyond those above, we consider now scenarios where user location sets posses some symmetry properties. This should also approximate (due to the continuity of the problem in user locations) scenarios where users are nearly-symmetric. We will need the following definitions of symmetric sets.

Definition 2: Let $\Omega_l = \{\boldsymbol{x}_n : n \in I_l\}$ be a set of $|I_l|$ points (users), where I_l is an index set and $|I_l|$ is its cardinality. The set Ω_l is called elementary symmetric if the distance between its center $\boldsymbol{a}_l = |I_l|^{-1}\sum_{n\in I_l}\boldsymbol{x}_n$ and any of its points is the same, i.e. $|\boldsymbol{a}_l - \boldsymbol{x}_n| = d_l \ \forall n \in I_l$.

Definition 3: Set Ω is symmetric if it is a union of disjoint elementary symmetric sets with the same centers, i.e. $\Omega = \cup_l \Omega_l$ and $\boldsymbol{a}_l = \boldsymbol{a} \ \forall l$.

While an elementary symmetric set is also symmetric, the converse is not true in general, i.e. a symmetric set does not need to be elementary symmetric, as Fig. 5 illustrates, so the former is more general than the latter. Equipped with these notions of symmetry, we are now able to obtain the optimal BS location in a closed form.

Proposition 3: Let the set Ω of user locations be symmetric, i.e. $\Omega = \cup_l \Omega_l$, where Ω_l are disjoint and elementary-symmetric, $\nu_n = \nu_l$ for any $n \in I_l$, and $\beta_n = \beta \ \forall n$. Then, for any pathloss exponents $\nu_n > 1$ for all n, the optimal BS location is its center $\boldsymbol{a}$, i.e. the average of the users' locations,

$$\boldsymbol{c}^* = \boldsymbol{a} = \bar{\boldsymbol{x}} = \frac{1}{N}\sum_n \boldsymbol{x}_n. \tag{44}$$

Proof: Since (6) is necessary for optimality of $\boldsymbol{c}^*$ and since optimal location is unique when $\nu_n > 1$, it is also sufficient, i.e. any $\boldsymbol{c}^*$ that satisfies (6) is optimal. We demonstrate below that $\boldsymbol{c}^* = \boldsymbol{a}$, where $\boldsymbol{a}$ is the center of Ω, does satisfy (6). Since all user locations form a union of elementary symmetric sets Ω_l of the same center $\boldsymbol{a}$, it follows that

$$\boldsymbol{a} = \frac{1}{N}\sum_n \boldsymbol{x}_n = \frac{1}{|I_l|}\sum_{i\in I_l}\boldsymbol{x}_i \tag{45}$$

Note that the distance $|\boldsymbol{a} - \boldsymbol{x}_i|$ between any user in Ω_l and its center $\boldsymbol{a}$ is the same, i.e. $d_l = |\boldsymbol{a} - \boldsymbol{x}_i|$ for any $i \in I_l$, since Ω_l is elementary symmetric. Using $\boldsymbol{c}^* = \boldsymbol{a}$ in 2nd part of (6),

$$\theta_i = \frac{|\boldsymbol{a} - \boldsymbol{x}_i|^{\nu_i - 2}}{\sum_n |\boldsymbol{a} - \boldsymbol{x}_n|^{\nu_n - 2}} = \frac{d_l^{\nu_l - 2}}{\sum_n |\boldsymbol{a} - \boldsymbol{x}_n|^{\nu_n - 2}} = p_l \ \forall i \in I_l \tag{46}$$

i.e. all weights θ_i are the same for all users in the same symmetric set Ω_l. Now using these θ_i in 1st part of (6), we obtain

$$\begin{aligned}\boldsymbol{c}^* &= \sum_n \theta_n \boldsymbol{x}_n = \sum_{I_l}\sum_{i\in I_l}\theta_i \boldsymbol{x}_i \\ &= \sum_{I_l} p_l \sum_{i\in I_l}\boldsymbol{x}_i = \sum_{I_l} p_l |I_l| \boldsymbol{a} = \boldsymbol{a}.\end{aligned} \tag{47}$$

as required, where the last 2 equalities are due to $\sum_{i\in I_l}\boldsymbol{x}_i = |I_l|\boldsymbol{a}$ and $\sum_n \theta_n = \sum_{I_l} \rho_l |I_l| = 1$. □

It should be emphasized that this result holds for any $\nu_n > 1$, not just for $\nu_n = 2$, as in Corollary 3, so this result is more general in terms of ν_n but more restrictive in terms of user locations as symmetry is required here, unlike Corollary 3. Note also that, unlike the general case, the optimal BS location is independent of pathloss exponent ν_n as long as the user set is symmetric. This Proposition also implies that when new users are added to existing ones, the optimal BS location is not affected as long as new users do not disturb symmetry.

E. CLUSTERING OF USERS

Let us consider a scenario when users are clustered around some points (social attractors, e.g. business or shopping centers, apartment buildings etc.), as illustrated in Fig. 6. When the cluster sizes (radii) are much smaller than the distance between them, then the optimal BS location can be approximated as follows. When only 2 clusters are present, their centers can be set, without loss of generality (via appropriate choice of the reference frame), to be $\boldsymbol{c}_1$ and $-\boldsymbol{c}_1$,

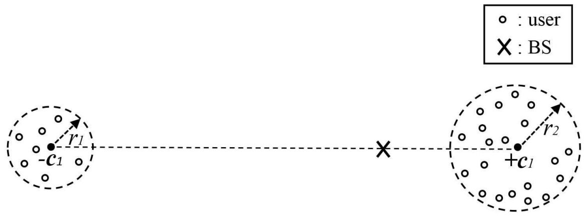

FIGURE 6. Users are clustered in two sets. An optimum location of the BS is approximated by (48).

and, choosing 1st basis vector along the same directions, the (scalar) coordinates are c_1 and $-c_1$.

Proposition 4: Let $\nu_n = \nu > 1$, $\beta_n = \beta$ for all n, and all the users be clustered in two sets, $\mathcal{C}_1$ and $\mathcal{C}_2$, and their cluster centers be $-\boldsymbol{c}_1$ and $\boldsymbol{c}_1$; let the distance between the clusters $D = 2|\boldsymbol{c}_1|$ be much larger that the cluster radii r_1 and r_2: $D \gg r_1, r_2$ (see Fig. 6). Then, the optimal BS location can be approximated as follows: it is on the line connecting the cluster centers and its coordinate c^* is

$$c^* \approx c_1 \frac{(m_2/m_1)^{1/(\nu-1)} - 1}{(m_2/m_1)^{1/(\nu-1)} + 1}, \tag{48}$$

where m_1 and m_2 are the number of users in each cluster.

Proof: When all users have the same parameters, $\beta_n = \beta\ \forall k$, the optimization problem (P2) in (4) is equivalent to

$$\min_{\boldsymbol{c}} \sum_n d_n^\nu, \tag{49}$$

Since the cluster sizes are much smaller than the distance between them, each cluster can be approximated by a point (located at its center) where all users of this cluster are located. Applying Corollary 1 under this approximation, the BS is located on the line segment connecting $\boldsymbol{c}_1$ and $-\boldsymbol{c}_1$, which is characterized by its coordinate c, so that $d_n \approx |c+c_1|$ for all users in $\mathcal{C}_1$, and $d_n \approx |c-c_1|$ for all users in $\mathcal{C}_2$. Under this approximation, the problem in (49) is simplified to

$$\min_c m_1|c+c_1|^\nu + m_2|c-c_1|^\nu, \tag{50}$$

Setting the derivative of the objective in (50) to zero, one obtains

$$m_1\nu(c+c_1)^{\nu-1} - m_2\nu(c_1-c)^{\nu-1} = 0, \tag{51}$$

from which (48) is obtained after some manipulations. □

Using this Proposition, we make the following observations.

1. c^* depends on m_2/m_1, c_1 and ν, but not on cluster sizes, provided that they are much smaller than the inter-cluster distance.

2. c^* is a monotonically-increasing function of m_2: if $m_2 > m_1$, then $c^* > 0$, i.e. the BS is closer to the bigger cluster centered at $c_1 > 0$, and it is getting closer to it as the number of its users grows.

3. If $m_1 = m_2$, then $c^* \approx 0$, i.e. the BS is in the middle of the clusters when they have the same number of users, which is an intuitively-appealing conclusion.

4. If $\nu = 2$, then

$$c^* \approx c_1(m_2-m_1)/(m_2+m_1) \tag{52}$$

5. Finally, if $m_2 \gg m_1$, then $c^* \approx c_1$, i.e. the BS approaches the bigger cluster center.

F. COLLINEAR USERS

In this section, we consider the case where all users are located on a line. This is motivated by practical settings on highways, in tunnels, street canyons or corridors. Following Corollary 1, an optimal BS location is also on the line, while its specific location depends on users' locations and path loss exponent. We consider below the case of $\nu_n = 1$ for all n and demonstrate some unusual properties such as non-uniqueness of optimal BS location. Note that $\nu < 2$ represents an environment more favorable for propagation than free space and it is possible in channels with guided wave structure, such as tunnels, corridors, street canyons [45].

Proposition 5: Let all users to have the same system parameters, $\nu_n = 1$, $\beta_n = \beta\ \forall n$, and be located on a line as represented by their scalar coordinates x_n, $n = 1 \ldots N$; without loss of generality, set $x_1 \le x_2 \le \ldots \le x_N$. If $\nu_n = 1$, an optimal BS location is a median of users' locations:

$$c^* = \begin{cases} x_{(N+1)/2}, & N \text{ is odd}, \\ \text{any } a \in [x_{N/2}, x_{N/2+1}], & N \text{ is even}. \end{cases} \tag{53}$$

Proof: Since all users as well as the BS are located on a line and transmission with the least per-user power is optimal, the problem (P2) is equivalent to

$$\min_c \sum_n |x_n - c|. \tag{54}$$

which is a convex problem. Since there are no constraints, the KKT conditions reduce to the stationarity condition (zero derivative at optimal point). When the number of users is even, consider any point a between two middle points, i.e. $x_{N/2} \le a \le x_{N/2+1}$, as illustrated in Fig. 7. Below, we demonstrate that this point is optimal. Indeed,

$$\begin{aligned} f(a) &= \sum_{n=1}^{N} |x_n - a| \\ &= \sum_{n=1}^{N/2}(a-x_n) + \sum_{n=N/2+1}^{N}(x_n - a) \\ &= \sum_{n=N/2+1}^{N} x_n - \sum_{n=1}^{N/2} x_n \end{aligned} \tag{55}$$

so that $df(a)/da = 0$ for any $a \in [x_{N/2}, x_{N/2+1}]$ and hence $c^* = a$. When the number of users is odd, consider any $a \in [x_{(N-1)/2}, x_{(N+1)/2+1}]$, so that

$$f(a) = |x_{(N+1)/2} - a| - \sum_{n=1}^{(N-1)/2} x_n + \sum_{n=(N+1)/2+1}^{N} x_n \tag{56}$$

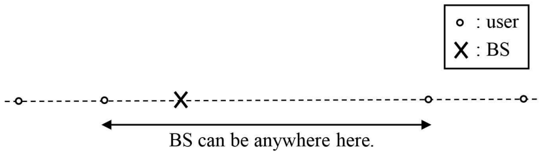

FIGURE 7. If $\nu_n = 1$ and the number of users is even, an optimal BS location is not unique: it can be anywhere between two middle-point users.

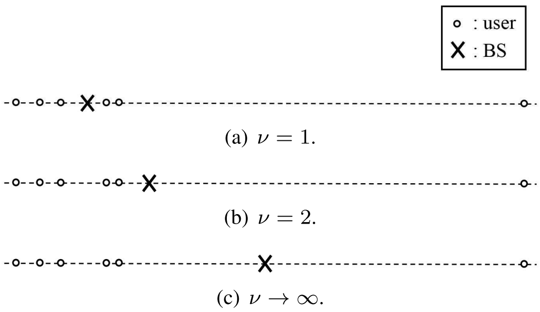

FIGURE 8. Optimum BS locations for different pathloss exponents. For $\nu = 1$, it is a median point, which is not unique (anywhere between users 3 and 4); for $\nu = 2$ - the average of the user locations; for $\nu \to \infty$ - the average of the most distant users. As ν increases, the impact of the distant user on the right increases too.

which is clearly minimized by $a = x_{(N+1)/2}$. It is straightforward to see that any a not in the interval $[x_{(N-1)/2}, x_{(N+1)/2+1}]$ cannot be optimal since it gives larger $\sum_n |x_n - a|$. Hence, $c^* = x_{(N+1)/2}$. □

An illustration of Proposition 5 is given in Fig. 7 when the number of users is even. Note that an optimal BS location is not unique in this case, which is ultimately due to the fact that $|x|$ is not strictly convex. However, if $\nu > 1$, then it is always unique, according to Proposition 1, since $|x|^\nu$ is strictly convex in this case. To see the impact of ν, let us consider 3 special cases as shown in Fig. 8:

1. For $\nu = 1$, an optimal BS location is a median point, which is not unique (can be anywhere between users 3 and 4).

2. For free-space propagation, $\nu = 2$, the optimal BS location is the (unique) average of the users' locations, according to Corollary 3.

3. For asymptotically-large ν, the optimal BS location is the average of the most distant users' locations, according to Proposition 2, so that most distant users contribute most to optimal BS location in this case.

Thus, ν has a profound impact on optimal BS location for asymmetric user sets. This is in stark contrast with symmetric user sets (Proposition 3), where the optimal BS location is independent of ν.

IV. ELEVATED BASE STATION

In practice, base station is often located at some elevation above ground to provide clear LOS to most users hence improving coverage. This also includes scenarios with an airborne communication node (e.g. a drone). To model this scenario, we consider the setting of Fig. 9, where users are located on a (ground) plane with 2-D vector $\boldsymbol{x}_n$ representing user n, while the BS is above the ground at a given height h and $\boldsymbol{c}$ is its 2-D location (projection) on the ground plane. The distance between the BS and user n is therefore $\sqrt{|\boldsymbol{c} - \boldsymbol{x}_n|^2 + h^2} = |\boldsymbol{c} - \boldsymbol{x}_n|_h$. Thus, the problem (P2) becomes

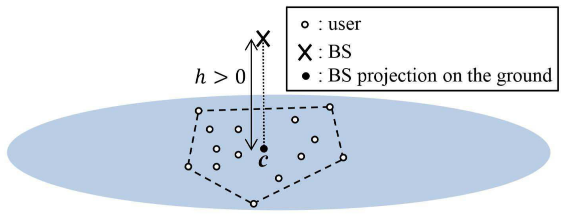

FIGURE 9. An elevated BS scenario, where all users are located on the ground plane while the BS is elevated to a given height h.

$$\min_{\{P_n\},\boldsymbol{c}} \sum_{n=1}^{N} P_n \text{s.t. } P_n \geq \beta_n |\boldsymbol{c} - \boldsymbol{x}_n|_h^{\nu_n} \tag{57}$$

The following Theorem characterizes its solutions.

Theorem 2: Consider the elevated BS location problem in (57) when $\nu_n \geq 1$. Its solution $\boldsymbol{c}^*$ can be expressed as a convex combination of user locations $\{\boldsymbol{x}_n\}$:

$$\boldsymbol{c}^* = \sum_n \theta_n \boldsymbol{x}_n, \ \theta_n = \frac{\beta_n \nu_n |\boldsymbol{c}^* - \boldsymbol{x}_n|_h^{\nu_n - 2}}{\sum_i \beta_i \nu_i |\boldsymbol{c}^* - \boldsymbol{x}_i|_h^{\nu_i - 2}}. \tag{58}$$

where $0 \leq \theta_n \leq 1, \ \sum_n \theta_n = 1$.

Proof: Follows from 2nd part of the proof of Theorem 1, see (13)-(19). □

Note that while Theorem 1 needs special consideration for singular cases, Theorem 2 is not restricted in this way, since $|\boldsymbol{x}|_h$ is differentiable for any $\boldsymbol{x}$ when $h \neq 0$. The characterization of $\boldsymbol{c}^*$ in Theorem 2 is similar, in its functional form, to that in Theorem 1, with the substitution $|\cdot| \to |\cdot|_h$. Hence, a number of properties/solutions pointed above also hold for the elevated BS problem in terms of its 2-D projected location $\boldsymbol{c}^*$. In particular, Corollaries 1-3, Propositions 2, 3, do hold for the elevated BS as well. Proposition 1 is strengthened as follows.

Proposition 6: The optimal elevated base station location is unique for any $\nu_n \geq 1$ if $h \neq 0$.

Proof: Follows the steps of that of Proposition 1 by observing that $|\boldsymbol{x}|_h^\nu$ is strictly convex for any $\nu \geq 1$ if $h \neq 0$. □

It is tempting to conclude that the optimal elevated BS location can be found by first solving the problem with $h = 0$ (no elevation) and then using its solution $\boldsymbol{c}^*$ and "elevating" it by h above the ground plane, but this is incorrect in general as shown by examples below. However, it is indeed the case if $\nu_n = 2$ for all n, as follows from (58).

V. ADDITIONAL LOCATION CONSTRAINTS

When locating a BS in practice, quite often there are some additional constraints due to existing infrastructure, such as a limited roof-top area available for a BS location. In such a case, the problem (P2) can be modified to include extra constraint on BS location as follows:

$$\text{(P3)}\ \min_{\{P_n\},\boldsymbol{c}} \sum_n P_n \ \text{ s.t. } P_n \geq \beta_n|\boldsymbol{c}-\boldsymbol{x}_n|^{\nu_n},\ |\boldsymbol{c}-\boldsymbol{a}_l| \leq r_l, \tag{59}$$

where $n = 1\ldots N$, $l = 1..L$; the additional constraints $|\boldsymbol{c}-\boldsymbol{a}_l| \leq r_l$ account for physical limitations or preferences, as discussed above, for given $\boldsymbol{a}_l$, r_l. Note that this formulation can also accommodate tethered UAVs, as in e.g. [23], [27] [28].

An optimal BS location under these extra constraints can be characterized as follows.

Theorem 3: When (i) $\nu_n \geq 2$, or/and (ii) $\nu_n \geq 1$ and $\boldsymbol{c}^* \neq \boldsymbol{x}_n$, the optimal BS location for the problem (P3) can be expressed as a convex combination of user and constraint locations:

$$\boldsymbol{c}^* = \sum_{n=1}^{N+L} \theta_n \boldsymbol{x}_n \tag{60}$$

where $\boldsymbol{x}_{N+l} = \boldsymbol{a}_l$,

$$\theta_n = \frac{\nu_n\beta_n|\boldsymbol{c}^*-\boldsymbol{x}_n|^{\nu_n-2}}{\sum_{n=1}^N \beta_n\nu_n|\boldsymbol{c}^*-\boldsymbol{x}_n|^{\nu_n-2} + 2\sum_{l=1}^L \mu_l}, \tag{61}$$

$$\theta_{N+l} = \frac{2\mu_l}{\sum_{n=1}^N \beta_n\nu_n|\boldsymbol{c}^*-\boldsymbol{x}_n|^{\nu_n-2} + 2\sum_{l=1}^L \mu_l}, \tag{62}$$

$n = 1\ldots N$, $l = 1\ldots L$, and dual variables $\mu_l \geq 0$ are found from

$$\mu_l(|\boldsymbol{c}^*-\boldsymbol{a}_l| - r_l) = 0 \tag{63}$$

subject to $|\boldsymbol{c}^*-\boldsymbol{a}_l| \leq r_l$. Signaling with the least per-user power is optimal: $P_n^* = \beta_n|\boldsymbol{c}^*-\boldsymbol{x}_n|^{\nu_n}$.

Proof: The proof is similar to that of Theorem 1. The Lagrangian is

$$L = \sum_n P_n + \sum_n \lambda_n(\beta_n|\boldsymbol{c}-\boldsymbol{x}_|^{\nu_n} - P_n) + \sum_l \mu_l(|\boldsymbol{c}-\boldsymbol{a}_l|^2 - r_l^2) \tag{64}$$

where $\mu_l \geq 0$ are Lagrange multipliers responsible for the additional location constraints. The stationarity condition is

$$\frac{\partial L}{\partial \boldsymbol{c}} = \sum_n \lambda_n\beta_n\nu_n(\boldsymbol{c}-\boldsymbol{x}_n)|\boldsymbol{c}-\boldsymbol{x}_n|^{\nu_n-2} + 2\sum_l \mu_l(\boldsymbol{c}-\boldsymbol{a}_l) = 0 \tag{65}$$

from which, after some manipulation, (60)-(62) follow. (63) are the complementary slackness conditions associated with $|\boldsymbol{c}-\boldsymbol{a}_l| \leq r_l$. □

Note that if $\mu_l > 0$ (active l-th location constraint), then $|\boldsymbol{c}^*-\boldsymbol{a}_l| = r_l$, i.e. an optimal BS location is on the circle of radius r_l centered at $\boldsymbol{a}_l$. Otherwise, the constraint is inactive and can be discarded. When all extra location constrains are inactive, $\mu_l = 0$ for all l and Theorem 3 reduces to Theorem 1.

Some of the properties above can be also extended to include additional location constraints. In particular, Proposition 1 applies verbatim and Corollary 1 is extended to $\boldsymbol{c}^* \in \textbf{conv}\{\boldsymbol{x}_n, \boldsymbol{a}_l\}$, i.e an optimal BS location is in the convex hull of $\{\boldsymbol{x}_n, \boldsymbol{a}_l\}$. Since $0 \leq \theta_n \leq 1$ and $\sum_n \theta_n = 1$, it follows from (60) that the optimal BS location is a weighted average of user locations and additional constraint centers.

If $\nu_n = 2$ and $\beta_n = \beta$, i.e. free-space propagation and identical user parameters,

$$\theta_n = \frac{\nu\beta}{\nu\beta N + 2\sum_l \mu_l},\ n = 1\ldots N, \tag{66}$$

$$\theta_{N+l} = \frac{2\mu_l}{\nu\beta N + 2\sum_l \mu_l},\ l = 1\ldots L, \tag{67}$$

so that the optimal BS location is the weighted average of the user locations and extra constraint centers.

VI. AN ITERATIVE ALGORITHM FOR THE GENERAL CASE

While a number of closed-form solutions of the location problem (P2) have been presented above, no such solution is known in the general case. However, the characterization of a solution in Theorem 1 can be exploited to build an iterative algorithm for the general case as follows. First, select an initial BS location $\boldsymbol{c}^1$ (not necessarily optimal) and use it in (6) to compute the weights θ_n. Second, use these weights to update the location according to the 1st equation in (6). The process can be repeated until some convergence condition is satisfied, as shown in Algorithm 1, where

Algorithm 1

1: **Initialization:** $i = 1$, $\boldsymbol{c}^1 = \sum_n \beta_n\boldsymbol{x}_n / \sum_n \beta_n$, $\epsilon > 0$.
2: **while** $|\boldsymbol{c}^{i+1} - \boldsymbol{c}^i| > \epsilon$ **do**
3: $\quad \boldsymbol{c}^{i+1} = f(\boldsymbol{c}^i)$.
4: $\quad i \leftarrow i+1$.
5: **end while**

$$f(\boldsymbol{c}) = \frac{\sum_n \beta_n\nu_n|\boldsymbol{c}-\boldsymbol{x}_n|^{\nu_n-2}\boldsymbol{x}_n}{\sum_n \beta_n\nu_n|\boldsymbol{c}-\boldsymbol{x}_n|^{\nu_n-2}}. \tag{68}$$

The convergence condition in line 2 of the algorithm can be substituted by some other suitable condition, for example, in term of the total BS power: $|P_T(\boldsymbol{c}^{i+1}) - P_T(\boldsymbol{c}^i)| < \epsilon$, where $P_T(\boldsymbol{c}) = \sum_n \beta_n|\boldsymbol{c}-\boldsymbol{x}_n|^{\nu_n}$ is the total BS power at location $\boldsymbol{c}$. Additional improvements of this basic algorithm are possible. For example, one can enforce a certain minimum number of iterations to ensure that the algorithm does not terminate prematurely. Additionally, one can select at each iteration the best overall location so far (it is sufficient to take the best of 2 most recent locations), in which case the sequence of total BS powers generated by the algorithm will be monotonically-decreasing.

When $\beta_n = \beta$ and $\nu_n = 1\ \forall n$, this algorithm coincides with Weiszfeld's algorithm [72] to solve the celebrated 350-years-old Fermat-Weber problem [71]. This problem as well as the algorithm have a long and convoluted history (including a number of false claims of convergence) [50]. Its convergence has been fully settled only recently [73].

It is beyond the scope of the present paper to study the convergence of Algorithm 1 in details. However, we do point out cases where such convergence is achieved in a single iteration. Numerical experiments below support the empirical conclusion that Algorithm 1 converges if $\nu_n \leq 3$.

Proposition 7: The Algorithm 1 converges in a single iteration, i.e. $\boldsymbol{c}^* = \boldsymbol{c}^2 = \boldsymbol{c}^1$*, if any of the following holds:*

1. $\nu_n = 2\ \forall n$.

2. The conditions of Proposition 3 hold.

3. There are 2 identical users, i.e. $\beta_1 = \beta_2$, $\nu_1 = \nu_2$.

4. $\boldsymbol{c}^1 = \boldsymbol{c}^*$*, i.e. initial location is optimal.*

Proof: To prove the last case, observe from (6) that using $\boldsymbol{c}^1 = \boldsymbol{c}^*$ in (68) results in $\boldsymbol{c}^2 = \boldsymbol{c}^1 = \boldsymbol{c}^*$ and hence the algorithm terminates in 1 iteration. Cases 1 - 3 follow from Case 4 since, in these cases, $\boldsymbol{c}^1 = \boldsymbol{c}^*$. □

Note that condition 4 implies that an optimal location $\boldsymbol{c}^*$ is a convergence point of the algorithm, i.e. if the algorithm reaches an optimal point, it will stop there.

This algorithm can also be used to solve the elevated BS location problem in (57), with the substitution $|\cdot| \rightarrow |\cdot|_h$ in (68). It is interesting to note that, in this case and when $\nu_n = 1$, $\beta_n = \beta\ \forall n$, the elevated BS problem coincides with that considered in [51], where $h \neq 0$ was introduced as a smoothing variable to avoid singularities and thus ensure the convergence of the barrier method. However, no physical justification for it was provided, beyond a computational convenience. In our setting, h appears naturally and has a solid meaning of the BS height above the ground plane.

VII. MULTI-BS LOCATION

In this section, we apply the above single-BS results to multi-BS location problem. Let us consider a scenario where a number of base stations form a cluster and each BS uses its own distinct set of frequencies, as typical in the cellular architecture [45]. This BS cluster is to serve a set of users with given locations and rate constraints. To accommodate multiple base stations and find their suitable locations, K-means algorithm (arguably, the most popular one) [52], [53], which finds applications in various fields and works well in many cases of practical importance, can be used [57], [58], [59]. This algorithm, however, is geometric in nature and was designed to group (abstract) data points into clusters based on some ad-hoc (arbitrary) "distance" metric (often, Euclidian distance is used, but other metrics are also possible), where, in the present setting, data points represent users and clusters represents cells and their "centers" - BS locations. Since various "distance" metrics are possible, a natural question arises: what is the best one and how to find it [52]? Note also that, in its original form, the K-means algorithm cannot ensure that the obtained BS locations and user clusters they form will minimize BS transmit power, even locally, subject to user rate constraints, since its ad-hoc "distance" metric (e.g. Euclidian, as in [57], [58], and [59]) is not related to the cellular system design.

To address these issues, we observe that the Tx power minimization problem (P2) in (4) is equivalent to

$$\min_{\boldsymbol{c}} \sum_n \beta_n |\boldsymbol{c} - \boldsymbol{x}_n|^{\nu_n} \tag{69}$$

since all inequalities hold with equality at an optimal point, see (32). Hence, it provides a natural physically-based measure of "distance" for n-th user in the form $\beta_n |\boldsymbol{c} - \boldsymbol{x}_n|^{\nu_n}$, which ultimately ensures, according to (3), (4) and (69), that the BS transmit power is minimized subject to user rate constraints and taking into account the propagation environment (via the path loss model). To extend this to multi-BS scenario, consider a setting where K BS located at $\boldsymbol{c}_k$, $k = 1..K$, serve N users located at $\boldsymbol{x}_n$, $n = 1..N$. Let B_k be a set of users served by k-th BS. Then, the total (sum) transmit power P_T of all BSs serving all users can be expressed as

$$P_T = \sum_{k=1}^{K} \sum_{\boldsymbol{x}_n \in B_k} \beta_{nk} |\boldsymbol{c}_k - \boldsymbol{x}_n|^{\nu_{nk}} \tag{70}$$

where ν_{nk} is the path loss exponent of user n when connected to BS k (here, we allow these path loss exponents to be different for different BS, as in e.g. multi-slope model [45] where path loss exponent depends on distance in a piece-wise constant manner; this reflects the possibility that LOS may be present for a path to some BS but not to another one). The objective here is to minimize P_T (subject to user rate constraints) via proper BS locations $\boldsymbol{c}_k$ as well as user-BS assignments B_k,

$$\min_{\boldsymbol{c}_k, B_k} \sum_{k=1}^{K} \sum_{\boldsymbol{x}_n \in B_k} \beta_{nk} |\boldsymbol{c}_k - \boldsymbol{x}_n|^{\nu_{nk}} \tag{71}$$

While, for fixed user-BS assignments B_k, this is a convex problem in $\boldsymbol{c}_k$, it is not overall convex, since the minimization over B_k is a combinatorial problem. Hence, it is difficult to solve in general (where "solve" means finding global optimum).[2] Using the physically-based "distance" measure $\beta_{nk} |\boldsymbol{c}_k - \boldsymbol{x}_n|^{\nu_{nk}}$ in the K-means algorithm, we propose the following Algorithm 1 to solve (71) locally. In this algorithm, $\boldsymbol{c}_k^{(t)}$ and $P_{Tk}^{(t)}$ are k-th BS location and its Tx power at iteration t, so that $P_T^{(t)} = \sum_k P_{Tk}^{(t)}$ is the total Tx power of all base stations at iteration t. In Step 2, users are assigned to base stations based on their "distance" measure $\beta_{nk} |\boldsymbol{c}_k^{(t-1)} - \boldsymbol{x}_n|^{\nu_{nk}}$ so that the Tx power needed to serve each user is minimized at this step via the user-BS assignment. In Step 3, the location of each BS is updated so that its total Tx power (to serve all users assigned to it) is also minimized. These 2 steps are repeated until convergence is reached. Several convergence criteria are possible: (i) stop if no new BS locations are found compared

[2] Globally-optimal solution is out of reach unless the number of users is very small, since this problem is NP-hard (exponential complexity), even in its simple form [54], [55], [56].

to the previous iteration, or (ii) if the reduction in the total Tx power $P_T^{(t)}$ is too small compared to previous iterations, or (iii) if t exceeds a maximum value of iterations t_{max}.

Algorithm 2 (Multi-BS location)

Require $\boldsymbol{c}_k^{(0)}$, β_{nk}, ν_{nk}, $k = 1..K$, $n = 1..N$.
1. Initialize: $t = 1$.
repeat
2. User-BS assignment: $B_k^{(t)} = \{\boldsymbol{x}_n : \beta_{nk}|\boldsymbol{c}_k^{(t-1)} - \boldsymbol{x}_n|^{\nu_{nk}} \leq \beta_{nm}|\boldsymbol{c}_m^{(t-1)} - \boldsymbol{x}_n|^{\nu_{nm}}\ \forall\, m \neq k\}$
3. Update BS locations: $\boldsymbol{c}_k^{(t)} = \arg\min_{\boldsymbol{c}} P_{Tk}^{(t)} = \sum_{\boldsymbol{x}_n \in B_k} \beta_{nk}|\boldsymbol{c} - \boldsymbol{x}_n|^{\nu_{nk}}$
4. $t := t + 1$
until convergence
5. Output: $\boldsymbol{c}_k^{(t-1)}$, $P_{Tk}^{(t-1)}$.

It is clear from the Algorithm description that it generates a non-increasing sequence $P_T^{(t)}$ (which is bounded from below) and hence converges (note that $P_T^{(t)}$ serves here as a Lyapunov function). However, its convergence point is not necessarily a global optimum - it may be just a local optimum and it may also depend on initial BS locations, which is a general property of the original K-means algorithm [52], [53], [54], [55], [56] and is not specific for its particular modification here. Note, however, that unlike the original K-means algorithm (which is geometric in nature and which make use of ad-hoc "distance" measure), Algorithm 1 is guaranteed to minimize (albeit locally) the total Tx power of all BSs to serve a given set of users subject to their individual rate constraints.

To partially overcome its local optimality and approach a global optimum, one can use a multi-start modification of this algorithm, i.e. to run it many times with different initial BS locations $\boldsymbol{c}_k^{(0)}$, possible choices of which include the following:

- randomly assign $\boldsymbol{c}_k^{(0)}$ to be equal to some user locations
- generate randomly $\boldsymbol{c}_k^{(0)}$ within given service area; alternatively, uniform or other grid can be used
- use some preferred locations (based e.g. on favorable propagation conditions, where LOS is available to most users, as in mmWave/THz 5G/6G systems)

Finally, we remark that extra location constraints, as in (59), can be easily accommodated in Step 3, and the constraints on the number of users assigned to each BS can also be included in Step 2. The above analytical results can be used at Step 3 to speed up the algorithm. Elevated BS, as in Sec. IV (Theorem 2), can also be considered by using $|\cdot|_h$ instead of $|\cdot|$ in Steps 2 and 3, and different BSs can have different heights as well.

VIII. NUMERICAL EXAMPLES

In this section, we validate and illustrate the analytical results above, examine their accuracy as well as the convergence of Algorithm 1. In all examples, users are located within a square of side $2R_{max}$ so that $|x_{in}| \leq R_{max}$; all coordinates are normalized (except for clustered scenarios) by R_{max} to make the results independent of physical size but dependent on geometry of user locations. To obtain clear insights, we separate the impact of user locations and propagation channel from that of the system-level parameters and set, in all examples, $\beta_n = \beta$ (where β_n absorbs all system-level parameters, as in (5)), and $\nu_n = \nu$, for all n. The total BS power P_T is normalized to βR_{max}^{ν}, so that the normalized

TABLE 1. The error norm $|c^* - c^*_{CVX}|$ averaged over 10^3 randomly-generated user sets.

$\lvert\boldsymbol{c}^* - \boldsymbol{c}^*_{CVX}\rvert$	5 users	10 users	50 users	100 users
$\nu = 1$	7.64E-06	7.95E-06	4.96E-06	5.42E-06
$\nu = 2$	1.36E-06	1.02E-06	1.14E-06	1.71E-07
$\nu = 3$	2.27E-06	1.48E-06	6.24E-07	2.33E-07
$\nu = 4$	5.78E-06	3.09E-06	1.62E-07	5.18E-08

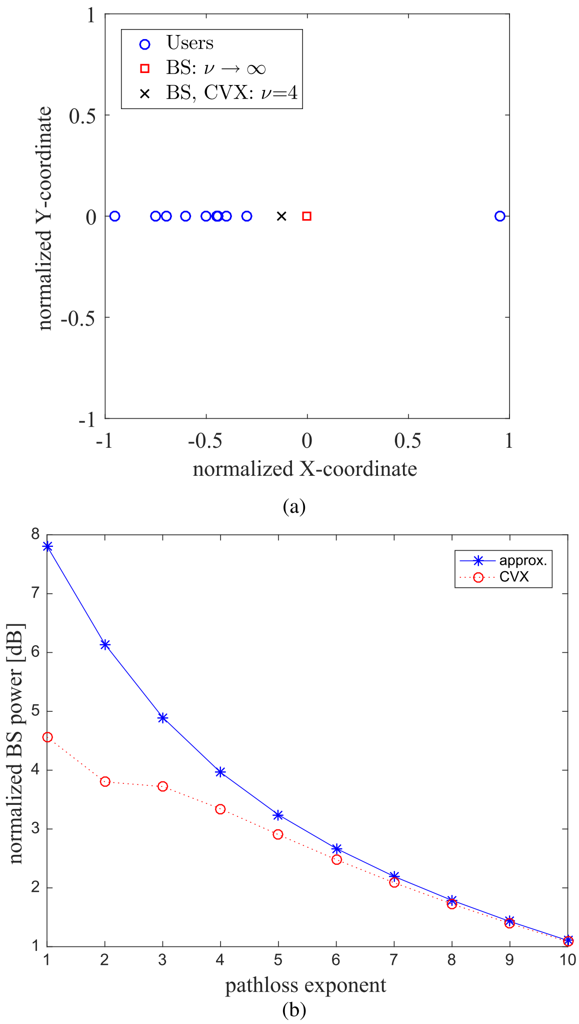

FIGURE 10. (a) User locations (asymmetric scenario) and optimal BS locations via the approximation (42) (for $\nu \to \infty$) and numerically via CVX for $\nu = 4$. The normalized BS powers are 3.96 and 3.34 dB, respectively, so that the approximation incurs only a small loss of 0.62 dB. (b) Normalized BS power vs. pathloss exponent ν for the user set in (a).

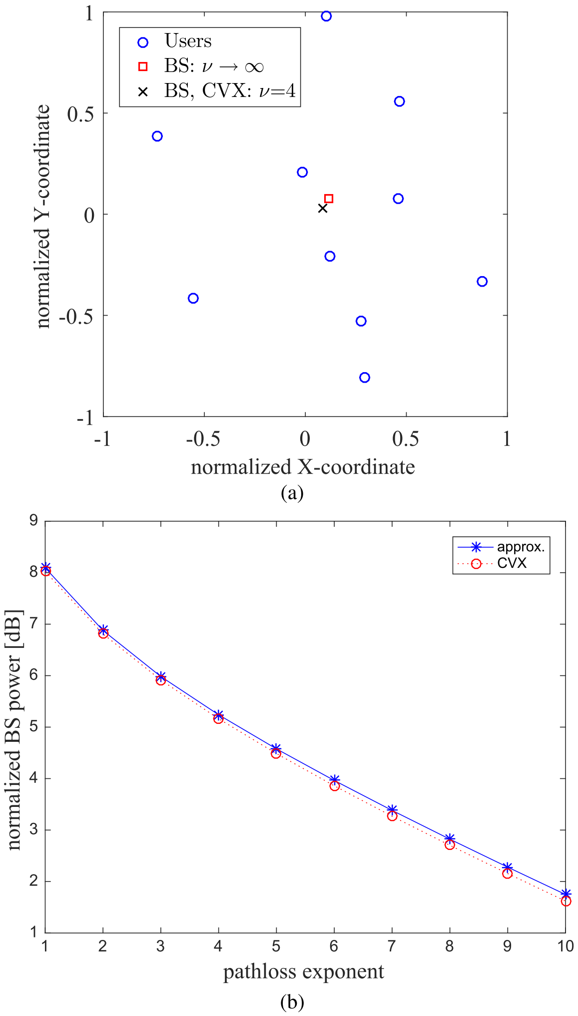

FIGURE 11. (a) User locations and optimal BS locations via the approximation in (42) and via the CVX, all for $\nu = 4$. (b) Normalized BS power vs. pathloss exponent for the user setting in (a). Note good agreement between the two for all considered values of ν.

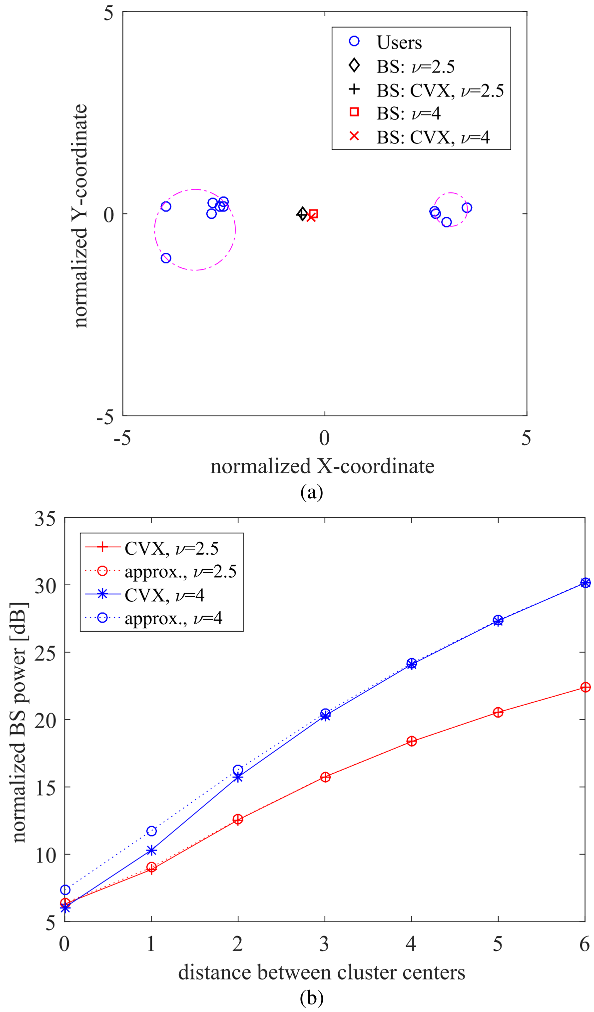

FIGURE 12. (a) Two clusters of users and optimal BS locations, found by (48) and by CVX, for $\nu = 2.5$ and $\nu = 4$; the cluster radii are 1 and 0.41. (b) Normalized BS power P_{Tn} vs. the inter-cluster distance for the setting in (a).

power

$$\widetilde{P}_T = \sum_n |\boldsymbol{c}^* - \boldsymbol{x}_n|^\nu / R_{max}^\nu = \sum_n |\widetilde{\boldsymbol{c}}^* - \widetilde{\boldsymbol{x}}_n|^\nu \tag{72}$$

where $\widetilde{\boldsymbol{c}}^*, \widetilde{\boldsymbol{x}}_n$ are normalized location vectors. Note that βR_{max}^ν is the BS power for a single user located at R_{max} distance from the BS, so that $\widetilde{P}_T$ [dB] is the excess power needed to serve all the users as compared to this single but most distant user located at cell edge. To simplify notations, we drop $\widetilde{(\cdot)}$ and use the original symbols $P_T, \boldsymbol{c}^*, \boldsymbol{x}_n$ to denote the normalized quantities below.

The expression for an optimal BS location in Theorem 1 was validated by comparing $\boldsymbol{c}^*$ in (6) with $\boldsymbol{c}^*_{CVX}$ obtained via the convex optimization toolbox CVX [39] to solve the problem (P2) in (4) numerically. In doing so, the optimal location $\boldsymbol{c}^*_{CVX}$ obtained numerically via CVX was used in 2nd equality in (6) to evaluate θ_k, which were subsequently used in 1st equality to evaluate $\boldsymbol{c}^*$. 10^3 user sets were randomly generated, where a given number of users were located with a unit square for each set, and the error norm $|\boldsymbol{c}^* - \boldsymbol{c}^*_{CVX}|$ averaged over all user sets was evaluated. No significant difference between $\boldsymbol{c}^*$ and $\boldsymbol{c}^*_{CVX}$ was observed for different path loss exponents and different numbers of users in each set. As Table 1 shows, the average error does not exceed 10^{-5} in all considered scenarios. The optimal BS location $\boldsymbol{c}^*$ was also compared with $\boldsymbol{c}^*_{CVX}$ for $\nu = 2$ (see Corollary 3) using 10^3 randomly-generated user sets as above. No significant difference was found either: in all tested cases, the average error did not exceed 10^{-5}.

Next, we assess the accuracy of the approximation in Proposition 2 (see (42)) when applied to finite ν, for asymmetric user locations in Fig. 10(a). Fig. 10(b) shows the normalized BS power P_{Tn} found via (42) and via CVX. Note a reasonably good agreement between the two methods, even when ν is not so large. When ν increases, the accuracy improves significantly. In many other tested cases, the convergence was much better. For example, Fig. 11(a) shows

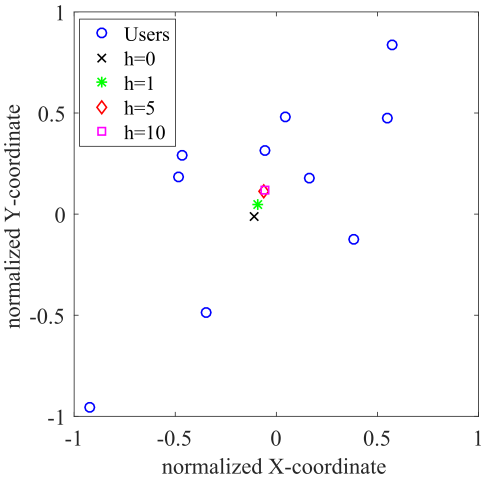

FIGURE 13. **The projection of the optimum BS location on the ground plane for different heights, $\nu = 4$. Note that the height affects the optimum ground location as well, but this effect is not significant if $h \geq 5$.**

a more symmetric user setting and optimal BS locations via (42) and CVX, while Fig. 11(b) shows the normalized BS power vs. ν. Note that the agreement here is much better than that in Fig. 10(b) for the whole considered range of ν. To understand this, observe from Proposition 3 that the optimal BS location is independent of ν if the user set is symmetric and, hence, nearly-independent if the set is nearly-symmetric (as in Fig. 11(a)), so that the actual BS power will be almost same for both BS locations (computed for a given ν and from Proposition 3).

Also note, from Fig. 11(b) and Fig. 10(b), that the normalized BS power in (72) decreases with ν, which indicates that these are the most distant users (at cell edge) that dominate for large ν. This is not the case for smaller ν, e.g. $\nu = 2$ as for LOS-dominated scenarios or $\nu < 2$ as for tunnel-type environments, where many users contribute to P_T, not only the most distant ones.

To validate the clustering approximation (48), Fig. 12(a) shows two clusters of users and optimal BS locations found via (48) and numerically by CVX, for $\nu = 2.5$ and $\nu = 4$. Note that the approximate and numerical solutions agree well with each other, even though the larger cluster size is not so small compared to the inter-cluster distance. The accuracy of approximation slightly decreases for larger ν. For the same clusters, Fig. 12(b) shows the impact of inter-cluster distance. The accuracy of the approximation in (48) increases with the distance; while it is uniformly good for $\nu = 2.5$, it is slightly worse for $\nu = 4$ when the distance is not large enough. Notice that the evaluation of optimal BS location based on the approximation in (48) is much simpler than that for the whole setting (for which no closed-form solution is known), hence demonstrating its usefulness. While in general the accuracy of the approximation depends on user locations, in addition to path loss exponent, good accuracy was observed in most tested cases.

Next, we consider an elevated BS location when all users are located on the ground. Fig. 13 shows the optimum BS location (projected on the ground) for $\nu = 4$ and various BS heights; $h = 0$ corresponds to no elevation. Observe that the projected optimal BS location is not the same as that with $h = 0$. Hence, finding an optimal BS location on the ground (no elevation) and then elevating it to height h is not optimal in general. Once certain hight is reached, its further increase does not have significant impact on optimal BS location.

IX. CONCLUSION

In this paper, unlike the known studies, the problem of determining an optimal base station location is formulated as a *convex* optimization problem to minimize the total BS power subject to QoS (rate) constraints. This brings in significant advantages: while only *sub-optimal* or *locally-optimal* solutions are available in the literature, *globally-optimal* solutions are obtained here, which are expressed as a convex combination of user locations. Based on this, a number of closed-form globally-optimal solutions are obtained, which reveal the impact of system and user parameters, propagation pathloss, as well as the overall system geometry. In particular, the optimal BS location is the average of users' locations in the case of unobstructed LOS propagation while in the case of large pathloss exponent (obstructed LOS), it is the average of the most distant users' locations and their weight increases with the pathloss exponent; when the pathloss exponent is unity, the optimal BS location is the median of users' locations. The symmetry in the user set was shown to make the optimal BS location independent of pathloss exponent, which is not true for asymmetric sets. These results provide insights unavailable from numerical algorithms, and allow one to develop design guidelines for more complicated systems. The single-BS results were extended to the multi-BS location problem (in a cell cluster) using a properly-modified form of the K-means algorithm with a physically-based distance measure, which (locally) minimizes the sum BS transmit power in a cell cluster via proper BS locations and user-BS allocation. Overall, the paper aims at building an analytical foundation for the BS location problem, that can facilitate system design and network planning, and can be further extended to include more complicated scenarios.

REFERENCES

[1] A. Taufique, M. Jaber, A. Imran, Z. Dawy, and E. Yacoub, "Planning wireless cellular networks of future: Outlook, challenges and opportunities," *IEEE Access*, vol. 5, pp. 4821–4845, 2017.

[2] E. Ayanoglu, "Guest editorial green communications and networking series," *IEEE J. Sel. Areas Commun.*, vol. 34, no. 12, pp. 3088–3091, Dec. 2016.

[3] S. Buzzi, I. Chih-Lin, T. E. Klein, H. V. Poor, C. Yang, and A. Zappone, "A survey of energy-efficient techniques for 5G networks and challenges ahead," *IEEE J. Sel. Areas Commun.*, vol. 34, no. 4, pp. 697–709, Apr. 2016.

[4] E. Amaldi, A. Capone, and F. Malucelli, "Planning umts base station location: Optimization models with power control and algorithms," *IEEE Trans. Wireless Commun.*, vol. 2, no. 5, pp. 939–952, Sep. 2003.

[5] S. Hurley, "Planning effective cellular mobile radio networks," *IEEE Trans. Veh. Technol.*, vol. 51, no. 2, pp. 243–253, Mar. 2002.

[6] C. Y. Lee and H. G. Kang, "Cell planning with capacity expansion in mobile communications: A Tabu search approach," *IEEE Trans. Veh. Technol.*, vol. 49, no. 5, pp. 1678–1691, Sep. 2000.

[7] X. Ling and K. Lawrence Yeung, "Joint access point placement and channel assignment for 802.11 wireless LANs," *IEEE Trans. Wireless Commun.*, vol. 5, no. 10, pp. 2705–2711, Oct. 2006.

[8] P. Gonzalez-Brevis, J. Gondzio, Y. Fan, H. V. Poor, J. Thompson, I. Krikidis, and P.-J. Chung, "Base station location optimization for minimal energy consumption in wireless networks," in *Proc. IEEE 73rd Veh. Technol. Conf. (VTC Spring)*, May 2011, pp. 1–5.

[9] X. Xu, W. Saad, X. Zhang, X. Xu, and S. Zhou, "Joint deployment of small cells and wireless backhaul links in next-generation networks," *IEEE Commun. Lett.*, vol. 19, no. 12, pp. 2250–2253, Dec. 2015.

[10] W. Zhao, S. Wang, C. Wang, and X. Wu, "Approximation algorithms for cell planning in heterogeneous networks," *IEEE Trans. Veh. Technol.*, vol. 66, no. 2, pp. 1561–1572, Feb. 2017.

[11] A. A. Khalek, L. Al-Kanj, Z. Dawy, and G. Turkiyyah, "Optimization models and algorithms for joint uplink/downlink UMTS radio network planning with SIR-based power control," *IEEE Trans. Veh. Technol.*, vol. 60, no. 4, pp. 1612–1625, May 2011.

[12] H. Ghazzai, E. Yaacoub, M.-S. Alouini, Z. Dawy, and A. Abu-Dayya, "Optimized LTE cell planning with varying spatial and temporal user densities," *IEEE Trans. Veh. Technol.*, vol. 65, no. 3, pp. 1575–1589, Mar. 2016.

[13] H. D. Sherali, C. M. Pendyala, and T. S. Rappaport, "Optimal location of transmitters for micro-cellular radio communication system design," *IEEE J. Sel. Areas Commun.*, vol. 14, no. 4, pp. 662–673, May 1996.

[14] Z. Ji, T. K. Sarkar, and B.-H. Li, "Methods for optimizing the location of base stations for indoor wireless communications," *IEEE Trans. Antennas Propag.*, vol. 50, no. 10, pp. 1481–1483, Oct. 2002.

[15] X. Cao, P. Yang, M. Alzenad, X. Xi, D. Wu, and H. Yanikomeroglu, "Airborne communication networks: A survey," *IEEE J. Sel. Areas Commun.*, vol. 36, no. 9, pp. 1907–1926, Sep. 2018.

[16] P. Yang, X. Cao, X. Xi, Z. Xiao, and D. Wu, "Three-dimensional drone-cell deployment for congestion mitigation in cellular networks," *IEEE Trans. Veh. Technol.*, vol. 67, no. 10, pp. 9867–9881, Oct. 2018.

[17] M. Alzenad, A. El-Keyi, F. Lagum, and H. Yanikomeroglu, "3-D placement of an unmanned aerial vehicle base station (UAV-BS) for energy-efficient maximal coverage," *IEEE Wireless Commun. Lett.*, vol. 6, no. 4, pp. 434–437, Aug. 2017.

[18] F. Lagum, I. Bor-Yaliniz, and H. Yanikomeroglu, "Strategic densification with UAV-BSs in cellular networks," *IEEE Wireless Commun. Lett.*, vol. 7, no. 3, pp. 384–387, Jun. 2018.

[19] E. Kalantari, H. Yanikomeroglu, and A. Yongacoglu, "Wireless networks with cache-enabled and backhaul-limited aerial base stations," *IEEE Trans. Wireless Commun.*, vol. 19, no. 11, pp. 7363–7376, Nov. 2020.

[20] E. Kalantari, "Base station placement in integrated aerial and terrestrial wireless cellular networks," Ph.D. thesis, School Elect. Eng. Comput. Sci., Univ. Ottawa, Ottawa, ON, Canada, 2020.

[21] E. Kalantari, S. Loyka, H. Yanikomeroglu, and A. Yongacoglu, "Optimal location of cellular base station via convex optimization," in *Proc. IEEE Int. Black Sea Conf. Commun. Netw. (BlackSeaCom)*, May 2020, pp. 26–29.

[22] J. Guo, P. Walk, and H. Jafarkhani, "Optimal deployments of UAVs with directional antennas for a power-efficient coverage," *IEEE Trans. Commun.*, vol. 68, no. 8, pp. 5159–5174, Aug. 2020.

[23] O. M. Bushnaq, M. A. Kishk, A. Celik, M.-S. Alouini, and T. Y. Al-Naffouri, "Optimal deployment of tethered drones for maximum cellular coverage in user clusters," *IEEE Trans. Wireless Commun.*, vol. 20, no. 3, pp. 2092–2108, Mar. 2021.

[24] Y. Liu, W. Huangfu, H. Zhou, H. Zhang, J. Liu, and K. Long, "Fair and energy-efficient coverage optimization for UAV placement problem in the cellular network," *IEEE Trans. Commun.*, vol. 70, no. 6, pp. 4222–4235, Jun. 2022.

[25] A. Gupta, A. Trivedi, and B. Prasad, "Deployment and trajectory design of fixed-wing UAVs in NOMA assisted wireless networks," *Phys. Commun.*, vol. 54, Oct. 2022, Art. no. 101789.

[26] H. Huang and A. V. Savkin, "Deployment of heterogeneous UAV base stations for optimal quality of coverage," *IEEE Internet Things J.*, vol. 9, no. 17, pp. 16429–16437, Sep. 2022.

[27] N. Cherif, W. Jaafar, E. Vinogradov, H. Yanikomeroglu, S. Pollin, and A. Yongacoglu, "iTUAVs: Intermittently tethered UAVs for future wireless networks," *IEEE Wireless Commun.*, vol. 30, no. 4, pp. 124–130, Aug. 2023.

[28] S. Khemiri, M. A. Kishk, and M.-S. Alouini, "Tethered UAV deployment strategies: The coverage and energy efficiency trade-off," *IEEE Open J. Commun. Soc.*, vol. 4, pp. 2561–2577, 2023.

[29] M. Nikooroo, O. Esrafilian, Z. Becvar, and D. Gesbert, "Optimization of placement and resource allocation in UAV-aided multihop wireless networks," *IEEE Internet Things J.*, vol. 11, no. 11, pp. 20051–20071, Jun. 2024, doi: 10.1109/jiot.2024.3369174.

[30] W. B. Heinzelman, A. P. Chandrakasan, and H. Balakrishnan, "An application-specific protocol architecture for wireless microsensor networks," *IEEE Trans. Wireless Commun.*, vol. 1, no. 4, pp. 660–670, Oct. 2002.

[31] V. Mhatre and C. Rosenberg, "Design guidelines for wireless sensor networks: Communication, clustering and aggregation," *Ad Hoc Netw.*, vol. 2, no. 1, pp. 45–63, Jan. 2004.

[32] J. Pan, L. Cai, Y. T. Hou, Y. Shi, and S. X. Shen, "Optimal base-station locations in two-tiered wireless sensor networks," *IEEE Trans. Mobile Comput.*, vol. 4, no. 5, pp. 458–473, Sep. 2005.

[33] M. Younis and K. Akkaya, "Strategies and techniques for node placement in wireless sensor networks: A survey," *Ad Hoc Netw.*, vol. 6, no. 4, pp. 621–655, Jun. 2008.

[34] G. Anastasi, M. Conti, M. Di Francesco, and A. Passarella, "Energy conservation in wireless sensor networks: A survey," *Ad Hoc Netw.*, vol. 7, no. 3, pp. 537–568, May 2009.

[35] E. Dahlman, S. Parkvall, and J. Skold, *5G NR: The Next Generation Wireless Access Technology*. London, U.K.: Academic Press, 2018.

[36] S. Boyd and L. Vandenberghe, *Convex Optimization*. Cambridge, U.K.: Cambridge Univ. Press, 2004.

[37] S. A. Vavasis, "Complexity issues in global optimization: A survey," in *Handbook of Global Optimization*, R. Horst and P. M. Pardalos, Eds. Boston, MA, USA: Springer, 1995, pp. 27–41.

[38] Y. Nesterov, *Lectures on Convex Optimization*, 2nd ed. Cham, Switzerland: Springer, 2018.

[39] M. Grant and S. Boyd. (Sep. 2013). *CVX: MATLAB Software for Disciplined Convex Programming*. [Online]. Available: http://cvxr.com/cvx

[40] J. M. Cioffi, G. P. Dudevoir, M. V. Eyuboglu, and G. D. Forney, "MMSE decision-feedback equalizers and coding. II. Coding results," *IEEE Trans. Commun.*, vol. 43, no. 10, pp. 2595–2604, Oct. 1995.

[41] G. D. Forney and G. Ungerboeck, "Modulation and coding for linear Gaussian channels," *IEEE Trans. Inf. Theory*, vol. 44, no. 6, pp. 2384–2415, Oct. 1998.

[42] C.-H.-F. Fung, W. Yu, and T. J. Lim, "Precoding for the multiantenna downlink: Multiuser SNR gap and optimal user ordering," *IEEE Trans. Commun.*, vol. 55, no. 1, pp. 188–197, Jan. 2007.

[43] J. Cioffi, *EE 379A—Digital Communication: Signal Processing*. Stanford, CA, USA: Stanford Univ., 2008.

[44] E. Arikan, D. J. Costello, J. Kliewer, M. Lentmaier, P. Siegel, R. Urbanke, and M. Pursley, "Guest editorial recent advances in capacity approaching codes," *IEEE J. Sel. Areas Commun.*, vol. 34, no. 2, pp. 205–208, Feb. 2016.

[45] T. Rappaport, *Wireless Communications: Principles and Practice*, 2nd ed. Upper Saddle River, NJ, USA: Prentice-Hall, 2001.

[46] *Study on Channel Model for Frequencies From 0.5 to 100 GHz*, document TR 38.901 V17.0.0, 3GPP, Mar. 2022.

[47] S. Sun, T. S. Rappaport, M. Shafi, P. Tang, J. Zhang, and P. J. Smith, "Propagation models and performance evaluation for 5G millimeter-wave bands," *IEEE Trans. Veh. Technol.*, vol. 67, no. 9, pp. 8422–8439, Sep. 2018.

[48] Y. Xing and T. S. Rappaport, "Propagation measurement system and approach at 140 GHz-moving to 6G and above 100 GHz," in *Proc. IEEE Global Commun. Conf. (GLOBECOM)*, Dec. 2018, pp. 1–6.

[49] Z. Shen, A. Khoryaev, E. Eriksson, and X. Pan, "Dynamic uplink-downlink configuration and interference management in TD-LTE," *IEEE Commun. Mag.*, vol. 50, no. 11, pp. 51–59, Nov. 2012.

[50] Z. Drezner and H. W. Hamacher, *Facility Location: Applications and Theory*. Berlin, Germany: Springer, 2002.

[51] K. D. Andersen, "An efficient Newton barrier method for minimizing a sum of Euclidean norms," *SIAM J. Optim.*, vol. 6, no. 1, pp. 74–95, Feb. 1996.

[52] D. MacKay, *Information Theory, Inference and Learning Algorithms*. Cambridge, U.K.: Cambridge Univ. Press, 2003.
[53] G. Gan, C. Ma, and J. Wu, *Data Clustering: Theory, Algorithms, and Applications*. Philadelphia, PA, USA: SIAM, 2007.
[54] M. Garey, D. Johnson, and H. Witsenhausen, "The complexity of the generalized Lloyd–max problem (Corresp.)," *IEEE Trans. Inf. Theory*, vol. IT-28, no. 2, pp. 255–256, Mar. 1982.
[55] D. Aloise, A. Deshpande, P. Hansen, and P. Popat, "NP-hardness of Euclidean sum-of-squares clustering," *Mach. Learn.*, vol. 75, no. 2, pp. 245–248, Jan. 2009.
[56] A. Vattani, "K-means requires exponentially many iterations even in the plane," *Discrete Comput. Geometry*, vol. 45, no. 4, pp. 596–616, Mar. 2011.
[57] J. Flathagen, Ø. Kure, and P. E. Engelstad, "Constrained-based multiple sink placement for wireless sensor networks," in *Proc. IEEE 8th Int. Conf. Mobile Ad-Hoc Sensor Syst.*, Oct. 2011, pp. 783–788.
[58] P. Sasikumar and S. Khara, "K-means clustering in wireless sensor networks," in *Proc. 4th Int. Conf. Comput. Intell. Commun. Netw.*, Nov. 2012, pp. 140–144.
[59] G. Y. Park, H. Kim, H. W. Jeong, and H. Y. Youn, "A novel cluster head selection method based on K-Means algorithm for energy efficient wireless sensor network," in *Proc. 27th Int. Conf. Adv. Inf. Netw. Appl. Workshops*, Mar. 2013, pp. 910–915.
[60] T. L. Marzetta, E. G. Larsson, and H. Yang, *Fundamentals of Massive MIMO*. Cambridge, U.K.: Cambridge Univ. Press, 2016.
[61] H. Q. Ngo, E. G. Larsson, and T. L. Marzetta, "Energy and spectral efficiency of very large multiuser MIMO systems," *IEEE Trans. Commun.*, vol. 61, no. 4, pp. 1436–1449, Apr. 2013.
[62] H. Q. Ngo, E. G. Larsson, and T. L. Marzetta, "Aspects of favorable propagation in massive MIMO," in *Proc. 22nd Eur. Signal Process. Conf.*, Sep. 2014, pp. 76–80.
[63] S. Rangan, T. S. Rappaport, and E. Erkip, "Millimeter-wave cellular wireless networks: Potentials and challenges," *Proc. IEEE*, vol. 102, no. 3, pp. 366–385, Mar. 2014.
[64] T. S. Rappaport, R. W. Heath Jr., R. C. Daniels, and J. N. Murdock, *Millimeter Wave Wireless Communications*. Upper Saddle River, NJ, USA: Prentice-Hall, 2015.
[65] T. S. Rappaport, Y. Xing, O. Kanhere, S. Ju, A. Madanayake, S. Mandal, A. Alkhateeb, and G. C. Trichopoulos, "Wireless communications and applications above 100 GHz: Opportunities and challenges for 6G and beyond," *IEEE Access*, vol. 7, pp. 78729–78757, 2019.
[66] H. Tataria, M. Shafi, A. F. Molisch, M. Dohler, H. Sjöland, and F. Tufvesson, "6G wireless systems: Vision, requirements, challenges, insights, and opportunities," *Proc. IEEE*, vol. 109, no. 7, pp. 1166–1199, Jul. 2021.
[67] A. N. Shiryaev, *Probability-2*, 3rd ed. New York, NY, USA: Springer, 2019.
[68] A. A. Borovkov, *Probability Theory*, 5th ed. London, U.K.: Springer, 2013.
[69] Y. V. Prohorov, *Law of Large Numbers, Encyclopedia of Probability and Mathematical Statistics*. Moscow, Russian: Encyclopedia, 2003.
[70] R. Lyons, "Strong laws of large numbers for weakly correlated random variables," *Michigan Math. J.*, vol. 35, no. 3, pp. 353–359, Jan. 1988.
[71] A. Beck and S. Sabach, "Weiszfeld's method: Old and new results," *J. Optim. Theory Appl.*, vol. 164, no. 1, pp. 1–40, Jan. 2015.
[72] E. Weiszfeld, "Sur le point lequel la somme des distances de N points donnds est minimum," *Tohoku Math. J.*, vol. 43, pp. 355–386, Jan. 1937.
[73] H. Üster and R. F. Love, "The convergence of the weiszfeld algorithm," *Comput. Math. Appl.*, vol. 40, nos. 4–5, pp. 443–451, Aug. 2000.

ELHAM KALANTARI received the Ph.D. degree in electrical and computer engineering from the University of Ottawa, in 2020. Her research interests include optimization, machine learning, resource management, O-RAN, and aerial networks. She was a recipient of the Ontario Graduate Scholarship, in 2019.

SERGEY LOYKA (Senior Member, IEEE) was born in Minsk, Belarus. He received the M.S. degree (Hons.) from the Minsk Radioengineering Institute, Minsk, in 1992, and the Ph.D. degree in radio engineering from Belorussian State University of Informatics and Radioelectronics (BSUIR), Minsk, in 1995. Since 2001, he has been a Faculty Member at the School of Electrical Engineering and Computer Science, University of Ottawa, Canada. Prior to that, he was a Research Fellow with the Laboratory of Communications and Integrated Microelectronics (LACIME), Ecole de Technologie Superieure, Montreal, QC, Canada; a Senior Scientist at the Electromagnetic Compatibility Laboratory of BSUIR, Belarus; and an Invited Scientist at the Laboratory of Electromagnetism and Acoustic (LEMA), Swiss Federal Institute of Technology, Lausanne, Switzerland. His research interests include information/communication theory, optimization, wireless communications and networks, and, in particular, MIMO systems and security aspects of such systems, in which he has published extensively. He received a number of awards from URSI, IEEE, Swiss, Belarus, and former USSR governments, and the Soros Foundation.

HALIM YANIKOMEROGLU (Fellow, IEEE) is currently a Professor with the Department of Systems and Computer Engineering, Carleton University, Ottawa, ON, Canada. His collaborative research with industry has resulted in 37 granted patents. His research interest includes 5G/6G wireless networks. He is a fellow of the Engineering Institute of Canada (EIC) and The Canadian Academy of Engineering (CAE). He received several awards for his research, teaching, and service, including the IEEE Communications Society Wireless Communications Technical Committee Recognition Award, in 2018, and the IEEE Vehicular Technology Society Stuart Meyer Memorial Award, in 2020. He was the General Chair of the IEEE VTC 2010-Fall, Ottawa, and VTC 2017-Fall, Toronto. He also served as the Chair for the IEEE Technical Committee on Personal Communications. He was the Technical Program Chair/Co-Chair of WCNC 2004, Atlanta, WCNC 2008, Las Vegas, and WCNC 2014, Istanbul. He is serving as the Chair for the IEEE Wireless Communications and Networking Conference (WCNC) Steering Committee. He is a Distinguished Speaker of the IEEE Communications Society and the IEEE Vehicular Technology Society.